



# Regional groundwater flow model for Abu Dhabi Emirate: scenario-based investigation

S. Sathish<sup>1</sup> · M. Mohamed<sup>1,2</sup>  · H. Klammler<sup>3</sup>

Received: 27 September 2017 / Accepted: 5 May 2018 / Published online: 31 May 2018  
© Springer-Verlag GmbH Germany, part of Springer Nature 2018

## Abstract

Despite the continuous increase in water supply from desalination plants in the Emirate of Abu Dhabi, groundwater remains the major source of fresh water satisfying domestic and agricultural demands. Groundwater has always been considered as a strategic water source towards groundwater security in the Emirate. Understanding the groundwater flow system, including identification of recharge and discharge areas, is a crucial step towards proper management of this precious source. One main tool to achieve such goal is a groundwater model development. As such, the main aim of this paper is to develop a regional groundwater flow model for the surficial aquifer in Abu Dhabi Emirate using MODFLOW. Up to our knowledge, this is the first regional numerical groundwater flow model for Abu Dhabi Emirate. After steady state and transient model calibration, several future scenarios of recharge and pumping are simulated. Results indicate that groundwater pumping remains several times higher than aquifer recharge from rainfall, which provides between 2 and 5% of total aquifer recharge. The largest contribution of recharge is due to subsurface inflow from the eastern Oman Mountains. While rainfall induced groundwater level fluctuation is absent in the western coastal region, it reaches a maximum of 0.5 m in the eastern part of the Emirate. In contrast, over the past decades, groundwater levels have declined annually by 0.5 m on average with local extremes spanning from 93 m of decline to 60 m of increase. Results also indicate that a further decrease in groundwater levels is expected in most of Emirate. At other few locations, upwelling of groundwater is expected due to a combination of reduced pumping and increased infiltration of water from nonconventional sources. Beyond results presented here, this regional groundwater model is expected to provide an effective tool to water resources managers in Abu Dhabi. It will help to accurately estimate sustainable extraction rates, assess groundwater availability, and identify pathways and velocity of groundwater flow as crucial information for identifying the best locations for artificial recharge.

**Keywords** Regional groundwater model · Abu Dhabi Emirate · Groundwater recharge and discharge · MODFLOW · UAE

## Introduction

In a hyper-arid region like Abu Dhabi, the importance of sustainable groundwater resources management to meet future freshwater demands is significant (Wheater et al. 2008). This is mainly due to the prolonged yield of groundwater,

its insensitivity to evaporation loss and the scarcity of surface water bodies. However, the regional groundwater study of Abu Dhabi Emirate conducted by the National Drilling Company and US Geological Survey reported that groundwater resources are under threat and will be scarce within few decades (USGS 1996). Declining groundwater levels over the recent decades have been attributed to increased pumping due to rapid growth in agricultural, forest and residential areas and reduced rainfall (Brook 2009; Sherif et al. 2011a, b; Mohamed and Almualla 2010a, b). Continued heavy pumping with limited or nil recharge may turn the aquifer sapless. Moreover, magnitude and duration of raised groundwater levels following recharge events depend on the aquifer's dynamic response properties. The balance between groundwater recharge to and discharge from the aquifer determines sustainability of aquifer exploitation. Hence, the

✉ M. Mohamed  
m.mohamed@uaeu.ac.ae

<sup>1</sup> National Water Center, United Arab Emirates University, Al Ain, United Arab Emirates

<sup>2</sup> Department of Civil and Environmental Engineering, College of Engineering, United Arab Emirates University, Al Ain, United Arab Emirates

<sup>3</sup> Engineering School for Sustainable Infrastructure and Environment (ESSIE), UF, Gainesville, FL, USA

management of groundwater resources based on an understanding of the aquifer's hydrogeological components and dynamics is important to avoid undesirable situations.

The presence of Falaj systems (Bronze aged canal system for water supply) in Abu Dhabi is an evidence for a long history of water resources management in the region. The recent drying-up of several Falaj systems further illustrates the decline in groundwater resources with respect to the past. The increase in groundwater pollution in Abu Dhabi (Mohamed et al. 2010a, b) has led to a decrease in agricultural productivity and undesirable social impacts (Miller et al. 2013; Zeng et al. 2016). In 2008, the United Nations (UN) reported that the available water resources per capita in the United Arab Emirates (UAE) are less than  $40 \text{ m}^3 \text{ year}^{-1}$ . This puts the Abu Dhabi Emirate (comprising 80% of UAE) among the regions with highest water scarcity worldwide. Several precaution measures are ongoing to avoid water scarcity in this typical hyper-arid region. As a part of current water resources management, groundwater pumping has been reduced year by year. To compensate, freshwater production from nonconventional sources, like desalination and treated sewage effluent (TSE), has been increasingly explored. Presently, the contribution of groundwater is negligible for domestic purposes, and mainly used for desert greenery [agriculture activities, forest development and amenities (parks and gardens)] activities with limited supply from desalination and TSE (SCAD 2011).

Likely to most of the desert environment in the world, the basin boundary of the study area is not remarkable other than the eastern part. The surface water is absent, and Wadies are non-perennial. The groundwater system is mainly controlled by geomorphic features: dune surface where groundwater level is mounded, gravel plain in the east which is the foothills of Oman Mountain so that recharge is high, and the flat coastal surface where rainfall recharge is completely nil with undesirable groundwater quality. An installation of aquifer storage and recovery, construction of dams, diversion of wadies and spring water, and application of groundwater recharge enhancing techniques are under the top concern in government sectors to avoid future water demand. Several pilot projects and investigations are being conducted to understand the subsurface behavior. However, there is also ambiguity in the understanding of regional hydrogeological system that results in to abnormal behavior while implementing precaution measures, i.e., sudden groundwater level rise, site-specific water logging, steep decline in the groundwater level, etc. Water introduced from nonconventional sources is known to partially enter the groundwater system by means of infiltration (Mohamed 2014). Over the past decades, in combination with reduced groundwater pumping rates has led to local rising of the groundwater level by as much as 60 m. Over the same time span, groundwater levels have locally declined by as much as 93 m at different

locations, where pumping has continuously increased. This combination of expanding nonconventional water sources and heavy pumping from the aquifer in different regions creates an uneven stress in this aquifer potentially causing complex dynamic responses over the long term. The regional groundwater model development will be a better solution to enhance long-term behavioral understanding of this hyper-arid aquifer. The drawbacks and future issues can be identified as prior using developed model. Jinyu et al. (2010) identified the suitable location of well fields using regional model of Yarkant basin sharing among Takelamagan desert, Buguli desert and Tuolulake Desert in the China. Abdulaziz and Faid (2015) used regional model to identify optimum groundwater pumping to control the water logging in the western desert of Egypt.

Numerical groundwater modeling is extensively applied at different scales to understand flow dynamics and solute migration, to forecast aquifer behavior, and to determine optimum pumping rates (Hassan and Mohamed 2003; Mohamed and Hatfield 2005; Mohamed et al. 2006, 2007; Konikow 2011; Sathish and Elango 2015; Siarkos and Latinopoulos 2016; Havril et al. 2017; Sathish and Mohamed 2018). Groundwater models based on advanced software programs are fundamental for the creation of regional hydrogeological databases and frameworks (conceptual models), for understanding the responses of aquifer systems to natural stresses and human interferences (abstraction and land use changes) and for the compilation of national groundwater atlases (Zhou and Li 2011; de Graaf et al. 2017; Alfaro et al. 2017). Regional linear/non-linear flow of groundwater, vertical and horizontal discontinuities of layers, variable layer thickness, and single to multilayer domains with steep topographic slopes can be modeled using MODFLOW (Gascuel Odoux et al. 2010; Zhou et al. 2014; Woodward et al. 2016). Gebreyohannes et al. (2017) developed a regional model for Geba basin and found out the groundwater pumping for irrigation activities is not driving from aquifer formation. The pumping takes place from the less conductive aquitard that will be drained out within a short-term period. Sahoo and Jha (2017) studied sensitiveness of groundwater flow to recharge and groundwater pumping from multilayer confined and unconfined aquifer at Mahanadi Basin, by a numerical approach using MODFLOW. MODFLOW 2005 (Harbaugh 2005) is a simple physical-based model using the finite difference approach and it provides flexibility in the handling of diverse multilayer and boundary conditions. Woodward et al. (2016) use a similar finite difference model for a catchment area possessing steep topographical slopes. Their objective was to analyze the patterns of non-linear catchment flow as a response to topography, precipitation and pumping of groundwater in the absence of internal catchment boundaries. Similar to their catchment, the Abu Dhabi aquifer is regionally interconnected and individual sub-basins

cannot be identified due to a lack of natural hydrogeological boundaries.

In the present study, we use MODFLOW 2005 to develop a regional groundwater model for Abu Dhabi Emirate based on existing hydrogeological information. This study is intended to help understanding and managing the groundwater system and its components in detail by providing authorities/decision makers with adequate information regarding the Abu Dhabi groundwater system and its interactions. As a result of these studies, site selection for the construction of recharge structures, the development of well fields, the enactment and reduction of desert greenery will be easily identified. Also, the developed model will motivate the generation of local scale groundwater flow models ranging from simple approximations to more elaborated models to simulate the behavior of this typical hyper-arid aquifers under different stress conditions. The model is calibrated and validated over periods of multiple years using recharge and groundwater pumping data collected by the Statistic Centre of Abu Dhabi (SCAD). It is not uncommon that the collected aquifer parameter required prior to groundwater modeling is not enough to represent the heterogeneity of the aquifer (Poeter and Hill 1997). The model complexity may extend beyond the available data. Hence, a sensitivity analysis is also conducted here to understand the response of the model to changes in aquifer parameters. Finally, the model is

applied to predict local variations in groundwater levels for different future recharge and pumping scenarios until 2030.

### Study area

The regional groundwater model is developed for the mainland of Abu Dhabi Emirate with an area of 67,340 km<sup>2</sup> (Fig. 1). The topographic elevation varies from mean sea level (MSL) of the Arabian Sea in the north to 1145 m above MSL near the Oman Mountains in the east. The aridity index shows that the area possesses hyper-arid climate (IPCC 2007) having a maximum temperature of 50 °C during the summer (June–August) and a minimum of 17 °C during the winter (December–February). The annual pan evaporation ranges between 3.4 and 4.4 m (Halcrow and Partners 1969). The mean annual precipitation varies between 100 mm in the east and 50 mm in the west. About 80% of precipitation occurs during the period from December through March. The humidity varies between 25% in the eastern part and 90% at the coast. The hydrodynamics of the eastern part is generally more transient due to various factors like higher rainfall recharge, drainage transmission loss from Oman Mountains and dense desert greenery.

The important geomorphological features that control the groundwater movement in the study area are the sand

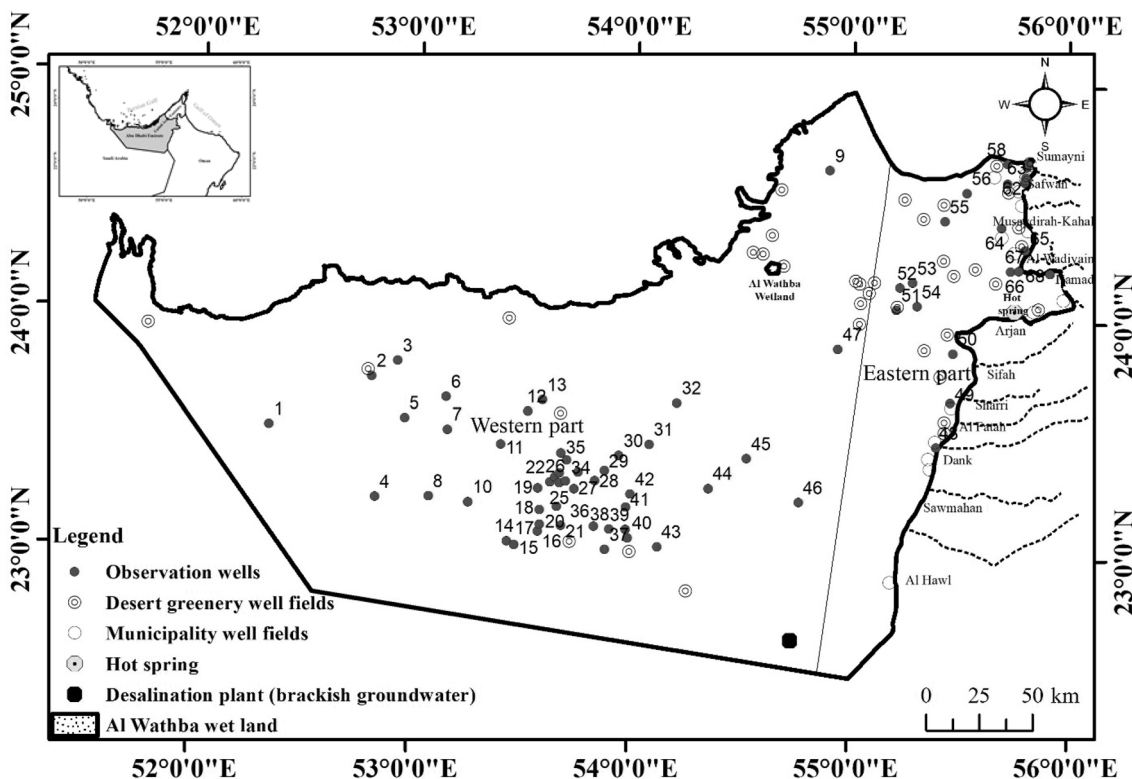


Fig. 1 Map of study area

dunes, 'Sabkha' flat terrain, piedmont plains, and the Jabal Hafit Mountain (Rizk and Alsharhan 2003). The linear and transverse types of sand dunes cover a large area in the centre with a maximum elevation of 259 m above MSL (Brook 2009). The entire area is limited by Sabkha towards the coast, which forms a transition zone between dunes and the Arabian Sea. The term Sabkha is locally used to represent a low hydraulic conductivity formation composed of calcareous silts and muddy sands. Also, several inland Sabkhas are present between the sand dunes. Sabkha Matti, the largest inland Sabkha extends from the coastal area and predominantly covers the western part of the study area. Piedmont plain occupies a large portion of the eastern part, and consist of the sediments derived from the Oman Mountains. The anticline Mountain Jabal Hafit trending NNW–SSE is composed of carbonate and evaporitic rocks such as limestone, dolomite, and gypsum (Elmahdy and Mohamed 2012, 2013a, b, 2014a, b, 2015a, b).

The pumping of groundwater in the entire region is monitored by the SCAD. Thousands of wells are in use for various purposes like desert greeneries, domestic needs and for one desalination plant (other plants use seawater). Among all, the groundwater is mainly used for desert greenery developments, i.e., agriculture, forests and parks. There are 39 well fields pumping water from shallow depths in the western part and shallow to deep depths in the eastern part. The number of wells in each well field varies from one to several hundreds depending on the size of the agriculture, forest, garden and park. Domestic well fields are active only in the eastern part and supplying 4% of water requirement. The groundwater-based desalination plant is located in the south-eastern part of the study area and pumps groundwater at a low rate to keep the desalination plant active.

## Geology and hydrogeology

The depth of the hard rock in the entire region is unexplored. Detailed subsurface investigations by the National Drilling Company (NDC), Groundwater Assessment Project (GWA) and United States Geological Survey (USGS 1996) report that the unconsolidated formation is composed of (1) Sabkha of Holocene age towards the coast and western part, (2) sand dunes and gravel of Holocene, Miocene and Pre-Quaternary age (palaeo sand dune) in the central and northeastern parts, (3) fluvial deposits of continental sandstone of Miocene age towards south and coast (Baynunah formation), (4) alluvial deposits that derived from Oman Mountain and Jabal Hafit of variable age towards the eastern part, and (5) spotted outcrop of weathered calcareous formation at the eastern boundary that trends parallel to the Oman Mountain. The collective of these geological units forms the surficial aquifer of the Abu Dhabi Emirate. The thickness of the surficial aquifer is largest in the central part with up to 60 m.

Depending on the location, the bottom of the surficial aquifer is bounded by (1) the lower Fars formation, (2) the upper Fars formation, and (3) tectonically disturbed marlstone and shales. In the eastern part towards the Oman Mountains, the bottom of surficial aquifer is underlain by upper Fars. However, the upper Fars is hydraulically connected to the surficial aquifer and also explored for groundwater pumping via deep wells. The western and most of the central areas of the surficial aquifer is underlined by lower Fars. This contradiction is due to a physiographic disturbance at the margin of the Arabian Peninsula, which uplifts lower Fars in the central and western part.

Hundreds of boreholes were drilled and pumping tests were conducted by NDC and USGS during the 1990s regional groundwater research project. Resulting data for hydraulic conductivity, effective porosity, and specific yield are used here as initial aquifer parameters. The hydraulic conductivity of the surficial aquifer varies between  $2.74 \times 10^{-8}$  and  $1.3 \text{ m day}^{-1}$  in the Sabkha formation of the coastal area and up to  $266 \text{ m day}^{-1}$  in the calcareous outcrops of the eastern part (Stanford and Wood 2001; USGS 1996). The hydraulic conductivity of unconsolidated sand and gravels varies from  $0.06$  to  $7.5 \text{ m day}^{-1}$  being lowest towards the south and highest towards the north. Specific yield is known to be highest in the calcareous outcrops in the east and the sand dunes with magnitudes of  $0.31$  and  $0.25$ , respectively.

For this regional groundwater model, three geological units are considered, namely surficial unconsolidated formations, upper Fars and lower Fars with thicknesses given in Table 1. Geological features below the lower Fars are not included in this study. An exception to this, there is a natural hot spring that seeps deeper groundwater onto the surface at a rate of  $2.5 \times 10^6 \text{ m}^3 \text{ year}^{-1}$  (Alsharhan et al. 2001) forming the surficial water body near Jabal Hafit Mountain in the east. In this model, also consider an artificial wetland of  $3.5 \times 1.5 \text{ km}$  with an average water column depth of  $0.74 \text{ m}$  (Al Dhaheri and Saji 2013). It is located towards the coastal boundary and connects to the Arabian Sea.

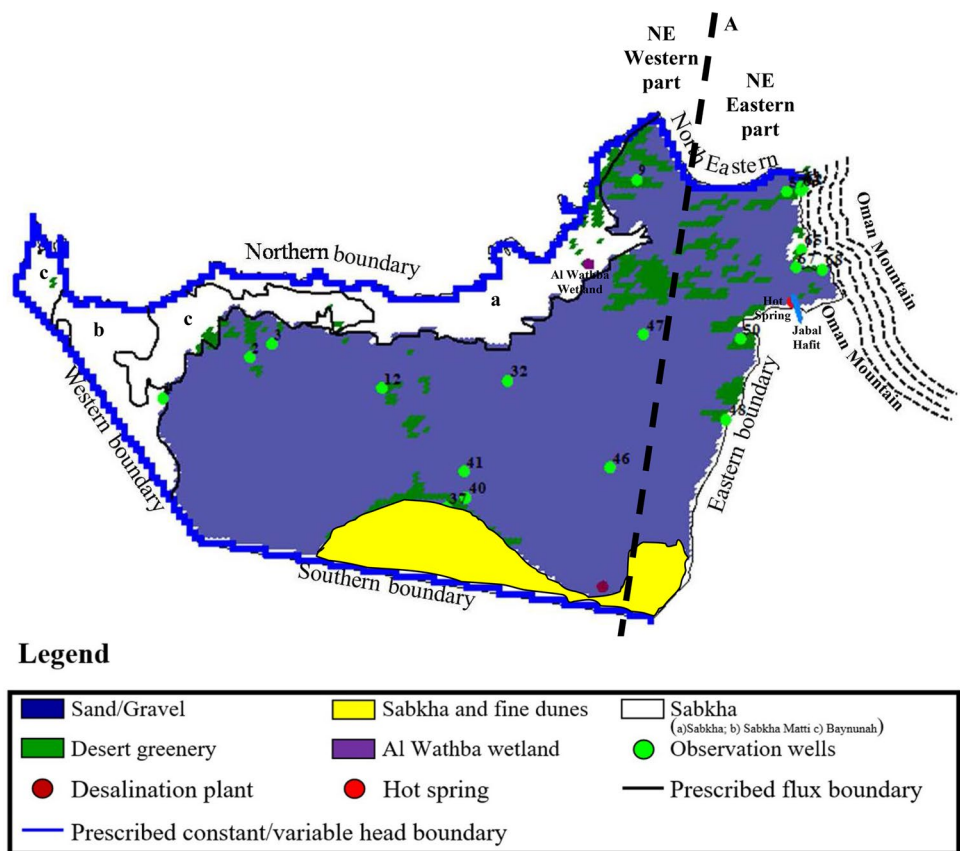
## Flow direction and boundary conditions

The coastline and the southern boundary allow groundwater to flow into the Arabic Sea and Saudi Arabia, respectively. The boundaries in the north-east and south-west are considered groundwater divides. Except for the eastern recharge boundary, all other boundary conditions in the model are defined as specified head boundary, using measured groundwater levels fluctuations (Fig. 2). These fluctuations possess a short-term (annual) component caused by rainfall recharge, and varying from  $0$  at the coastal boundary to  $0.5 \text{ m}$  in the eastern part. Apart from this, there are long-term declines and rises in groundwater levels between  $-0.06$  and  $0.33$

**Table 1** Subsurface lithology

Model layer	Western part			Eastern part		
	Formation	Thickness (m)	Purpose of pumping	Formation	Thickness (m)	Purpose of pumping
1	Surficial unconsolidated formation [Sabkha, sand dunes, fluvial deposits (Baynunah formation)]	60	Desert greenery	Surficial unconsolidated formation (Sabkha, sand dunes, alluvial deposits, weathered calcareous formation)	50	Desert greenery, domestic use, desalination plant
				Upper Fars		
2	Lower Fars	160–200	NA	Lower Fars	150	NA

**Fig. 2** Aquifer boundaries and partition representing spatial variation in rainfall (Brook 2009; Shahid et al. 2013)

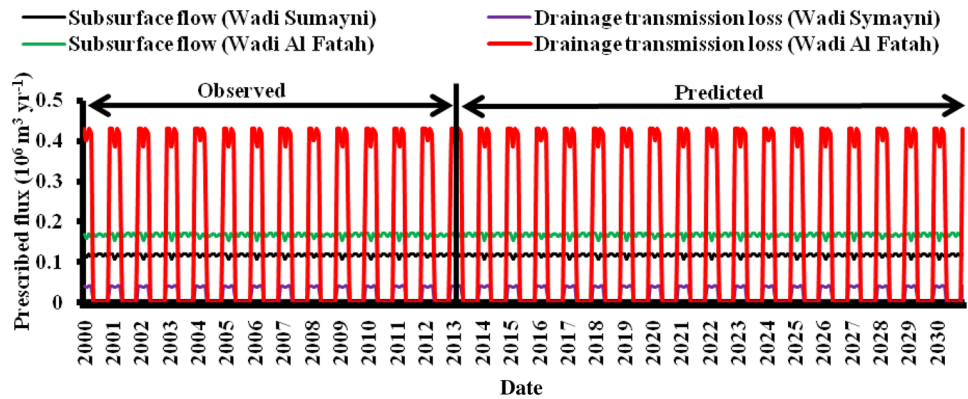


m year<sup>-1</sup>, which are highly localized at the north eastern boundary. Natural discharge of groundwater into the sea is usually controlled by the tidal difference and hydraulic conductivity of coastal aquifer (Brook 2009). In this case, however, discharge into the sea is very low due to the low hydraulic conductivity of Sabkha, such that tidal variability is neglected and the coast is considered as a prescribed constant head boundary.

Based on potentiometric maps of the Abu Dhabi aquifer and its surroundings, it is known that the eastern boundary receives recharge from subsurface flow. Twelve recharge

basins bordering the eastern boundary of the modeled area contribute to recharge at different degrees depending on the catchment area, drainage length, slope and soil matrix. Moreover, drainage transmission losses occur at five drainage channels during the period of monsoon between December and April near the northern and central portions of the eastern boundary. Due to the channel’s proximity to the eastern boundary, subsurface recharge and transmission losses are considered as recharge rates (MWR 1999) across the eastern boundary with magnitudes specified in Fig. 3.

**Fig. 3** Prescribed flux of subsurface flow and drainage transmission loss of selected drainages at eastern boundary used in the development of model (MWR 1999)



**Conceptual model**

Grid size and temporal resolution directly impact the model outcomes and are limited by the total area and time period under consideration. A monthly resolution is chosen, for which rainfall data is available and which allows investigating seasonal variability. As shown in Fig. 4, the total study area of 67,340 km<sup>2</sup> is discretized into cells of 3 km<sup>2</sup> with centered nodes, covering a total of 154 columns and 92 rows in the horizontal plane. This is the result of a trial and error approach and deemed a reasonable compromise between computational efficiency, successful model convergence and spatial resolution with respect to piezometric gradients as well as the scales of hydrogeological heterogeneity. The use of block centered

nodes and the absence of steep hydraulic gradients favor minimization of errors near the model boundaries. Just outside the eastern boundary, one additional grid row is used for assigning subsurface recharge. The number of layers can be decided by the presence of discontinuity in the geological unit or hydrogeological unit. In several situations, especially in regional models, a number of geological layers and hydrogeological layers are not same. Brook (2009) reported three geological layers, namely (1) surficial aquifer (2) upper fars and (3) lower fars (Fig. 5). The regional hydrogeological investigation carried out by USGS (1996) reported the same, but in most of the places, especially towards eastern part, upper fars has a hydrogeological connection with the surficial aquifer. The surficial aquifer is very thin and absent in several places of the eastern part. Several boreholes have screening in

**Fig. 4** Conceptualization of the Abu Dhabi aquifer for regional groundwater model

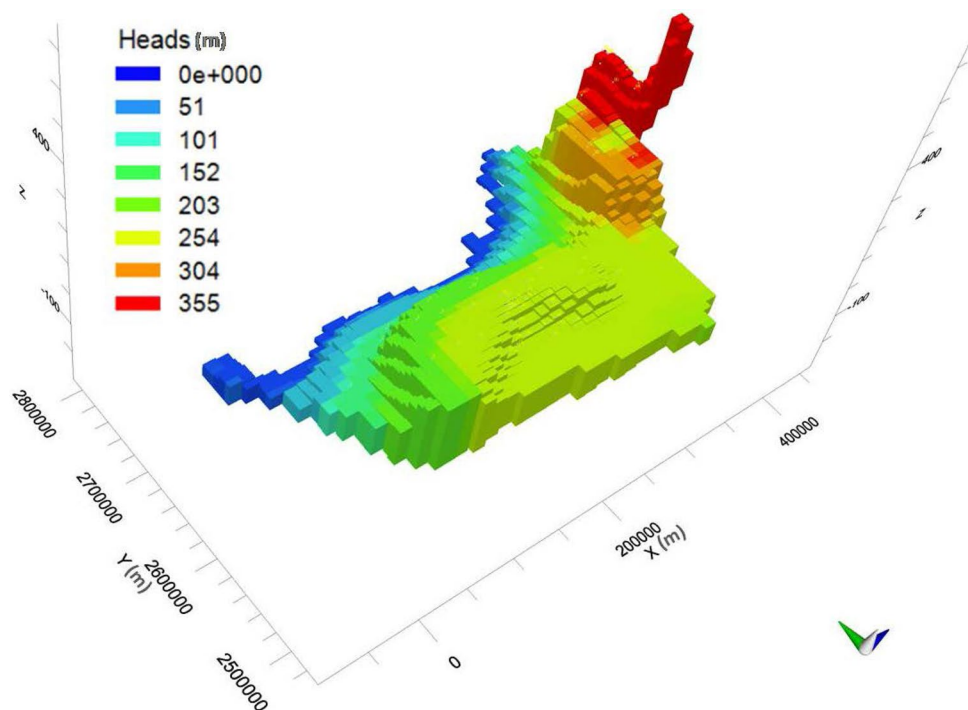
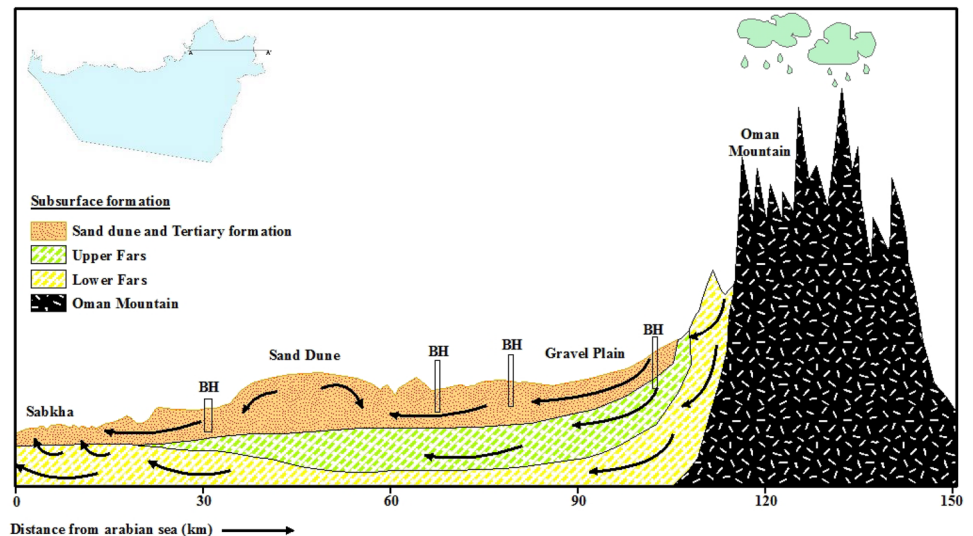


**Fig. 5** Conceptualized subsurface cross-section of Abu Dhabi (after Alsharhan et al. 2001)



both formations without causing a piezometric effect. Due to the hydrogeological connection of upper fars and the surficial aquifer in the east, and the absence of upper fars in the central and western parts, the upper fars and the surficial aquifer are conceptualized as a single layer. The thickness of this first layer varies from 5 m in the coastal shoreline to 900 m in the eastern boundary. The lower fars is considered as a second grid layer forming the base of the aquifer (Table 1). The thickness of the lower fars varied from 150 m in the east to 200 m in the western part. The model was executed from January 2000 to December 2030 with a total of 372 monthly stress periods used for calibration, validation and prediction of future scenarios.

The topography, recharge and discharge of groundwater, lateral boundary conditions, and bottom of the aquifer are the main factors controlling the behavior of a three dimensional regional groundwater flow model (Saroli et al. 2017; Todd 1980). To maintain the reliability of the model, recharge was calculated as per universal standard methods. Moreover, topography data extracted from digital elevation model of Shuttle Radar Topographic Mission (SRTM DEM) was employed to reduce the error in groundwater flow caused by elevation difference. The annual rate of discharge of groundwater monitored by SCAD is employed. Due to hyper-arid climate condition, the time schedule of pumping and the rate of pumping remains the same. Hence, the spatial distribution of the rate of discharge from greenery well fields and domestic wells was able to understand efficiently on the basis of distribution of desert greenery area and domestic wells, and can develop the model using the monthly stress period. The use of automated layer type (convertible) in the MODFLOW (Harbaugh 2005) forms the existing natural condition either confined or unconfined status of the bottom layer based on groundwater level elevation. The model with block centered flow package and layer type three allows

variable transmissivity and storage. The model with this layer type is convertible between confined and unconfined condition automatically on the basis of aquifer parameter, geometry and saturation of the model layer. Transmissivity will be recalculated on each iteration using above variables. Storage term and vertical flow will be automatically implemented. This enables a realistic prediction, especially in the aquifer portion along the coastal Sabkha. Along the coastal boundary, the lower conductivity Sabkha overlies the higher conductivity lower Fars of the bottom layer. This results in a confined aquifer system and produces seepage of groundwater along the coastal Sabkha.

## Wetland discharge and pumping

The artificial wetland at Al Wathba is located in the northern part of the study area with a size of  $3.5 \times 1.5$  km. The average bottom elevation above MSL and depth of water body are 16.5 and 0.74 m, respectively. This is assigned as a constant pond stage in the model, which is the product of the balance between evaporation and inflow from surrounding groundwater, TSE and natural runoff from adjacent agricultural lands (ERWDA 2001; Al Dhaheri and Saji 2013).

The spatial extent of desert greenery has remained relatively constant in the eastern part, while it has increased at an average annual rate of 3.9% in the western part of the study area. The water requirement for each square kilometer of greenery varies on the basis of the plant types. The average annual groundwater pumping per square kilometer of greenery area was calculated using the volume of groundwater pumping from individual well fields (SCAD 2011; Brook 2009) and the total area of greenery (SCAD 2011; EAD 2012). This was done separately for the eastern and western parts resulting in averages of  $3.29 \times 10^6 \text{ m}^3 \text{ year}^{-1} \text{ km}^{-2}$  in

the eastern part and  $3.95 \times 10^6 \text{ m}^3 \text{ year}^{-1} \text{ km}^{-2}$  in the western part (Table 2). The monthly pumping rates of groundwater based on area of desert green activities were calculated and used in the model distributed over total area of desert green (Fig. 6). A slight reduction in pumping rate is observed from 2004 to 2008 due to the increase of the contribution of desalinated water and TSE water. The pumping of groundwater for the domestic purpose is limited to the eastern part and has been reduced to  $10 \times 10^6 \text{ m}^3 \text{ year}^{-1}$  (Brook 2009). The additional amount of water for domestic purposes is supplied from desalination plants. The extraction of groundwater from the desalination plant located in the south-eastern part is  $49.77 \times 10^6 \text{ m}^3 \text{ year}^{-1}$ .

## Rainfall and infiltration

The Abu Dhabi aquifer is mainly recharged by subsurface inflow through the eastern boundary. Unlike for aquifers in more humid regions, rainfall represents a much less significant portion of recharge (Dougherty et al. 2009). However, it is reported that rainfall recharge ranges between 2 and 10% of rainfall and is capable of covering 4% of the total annual water consumption (Osterkamp et al. 1995; Khalifa 1995; Rizk and Alsharhan 2003; Healy 2010). Rainfall in Abu Dhabi shows huge spatial and temporal variations that may impact the long-term regional responses of the aquifer (Sherif et al. 2011b). Thus, rainfall recharge was estimated using data obtained from 12 rain gauge stations at various locations. The rainfall varied from 50 to 100 mm with 80% of the rainfall occurring between the months of November and March. The highest rainfall is always noticed towards the eastern part because of the higher altitude mountains. To capture some of this spatial heterogeneity in rainfall, recharge  $R$  was estimated separately for the eastern and western parts of the study area. The one-dimensional groundwater level fluctuation method was employed at locations with measurements of specific yield  $S_y$  and observations of changes in groundwater level elevation  $\Delta h$  over time intervals  $\Delta t$  from

$$R = S_y \Delta h / \Delta t. \quad (1)$$

This method of estimation disregards the mechanism by which water moves through the unsaturated zone or horizontally through the aquifer (Healy and Cook 2002; Jassas and Merkel 2014).

The observation wells located away from desert green activities are employed in this calculation. In response to an average rainfall of 69 mm in the year 2009–2010, wells located outside agriculture fields shows an average increase of 0.5 m in the eastern part and 10 mm in the western part other than coastal Sabkha. According to Eq. 1, this corresponds to 5 and 2% of rainfall infiltrating as recharge into the

aquifer for both parts of the study area. In the coastal Sabkha region, the increase of groundwater level was not noticed in the wells indicating a nil rainfall recharge as reported previously by Stanford and Wood (2001).

The withdrawals of groundwater for desert greenery activities are monitored by the SCAD (Table 2). The gross irrigation water demand (including transportation losses and application losses) and the contribution of nonconventional sources of water are monitored annually by the SCAD. Both transportation and application losses are persistent and different in volume among the types of irrigation system, and directly alter the rate of irrigation return flow (Gates et al. 2012). Irrigation return flow depends on irrigation method, but also on soil type, irrigation depth and crop rooting size (Howell 2003). The micro irrigation system is dominantly used in the Abu Dhabi irrigation development, as it causes significantly less transportation and application losses than surface systems. Irrigation return flow  $R_{ir}$  is calculated as

$$R_{ir} = (1 - E_c E_a) Q_{ir}, \quad (2)$$

where  $Q_{ir}$  is gross irrigation water demand ( $\text{m}^3 \text{ year}^{-1}$ ) known from total contribution of groundwater, TSE and desalination water to the desert greenery development (Table 2; Fig. 6). The coefficients  $E_c = 0.95$  and  $E_a = 0.9$  are nation-wide conveyance and application efficiencies, respectively (PIK 2007).

With this, the irrigation return flow is calculated and also predicted until the period of model simulation as uniformly distributed magnitudes over greenery areas (Table 2). The recharge induced by the irrigation return flow and infiltration of the nonconventional source of water in the western part of the study area is several times higher than the recharge caused by rainfall.

## Model calibration and validation

Model calibration is divided into two parts for steady and transient state using constant and time-dependent input parameters, respectively. The decision of using a transient model or investigation only with steady state model depends on the aquifer response. The response of the aquifer to recharge and discharge will help to proceed further either into transient model or to end up with steady state model. Townley (1995) and Haitjema (2006) presented that, if an aquifer does not respond well to recharge and discharge, then the use of a steady state model with averaged boundary conditions would produce good results. In the present work, a transient model was necessary because the aquifer is responding to the recharge in the eastern part, since this part receives more rainfall and Wadi's transmission loss. Hence, this part is more active than the west in the event of recharge and discharge. Towards western part, the response



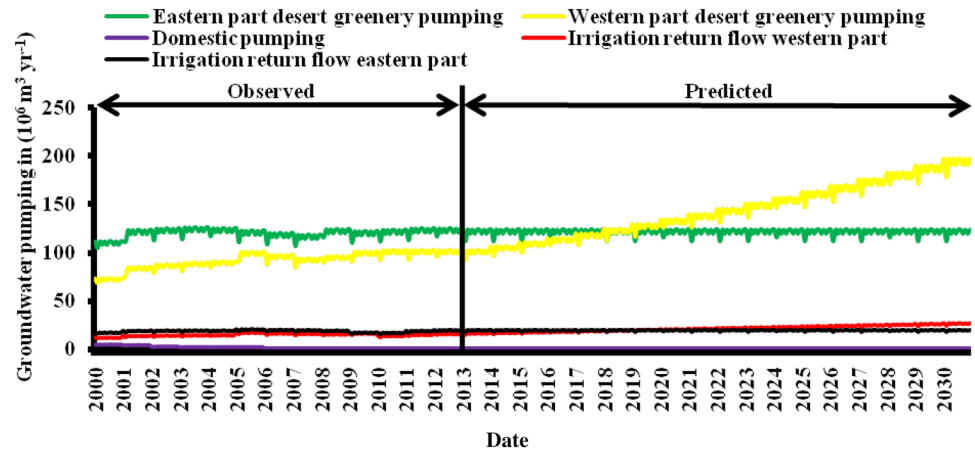
**Table 2** Spatial and temporal changes of desert greenery area, groundwater pumping rates, irrigation return flow, TSE, desalination water and boundary condition per year (SCAD 2011; EAD 2012)

Year	Western zone		Eastern zone		Western zone		Eastern zone		Western zone		Eastern zone		Western zone		Eastern zone		Domestic pumping in ( $10^6 \text{ m}^3 \text{ year}^{-1}$ )	Transient change in head at boundary in (MSL)		Total flux at eastern boundary in ( $10^6 \text{ m}^3 \text{ year}^{-1}$ ) east			
	field ( $\text{km}^2$ )	zone	zone	zone	zone	zone	zone	zone	zone	zone	zone	zone	zone	zone	zone	zone		North-east	Coastal boundary, south and west				
Total area of greenery field ( $\text{km}^2$ )		Total pumping rate in ( $10^6 \text{ m}^3 \text{ year}^{-1}$ ) <sup>a</sup>		TSE in ( $10^6 \text{ m}^3 \text{ year}^{-1}$ ) <sup>b</sup>		Desalination water in ( $10^6 \text{ m}^3 \text{ year}^{-1}$ ) <sup>b</sup>		Gross irrigation water demand ( $Q_{ir}$ ) in ( $10^6 \text{ m}^3 \text{ year}^{-1}$ )		Irrigation return flow $R_{ir}$ ( $10^6 \text{ m}^3 \text{ year}^{-1}$ )		Eastern zone		Western zone		Eastern zone		Western zone		Eastern zone			
2000	220	400	869	1316	71	32	3	8	943	1356	141	203	58	0 to 0	0 to 0	0 to 0	0 to 0	0 to 0	0 to 0	0 to 0	0 to 0	38.5	
2001	254	441	1003	1451	71	32	4	10	1078	1493	162	224	51	0 to 0	0 to 0	0 to 0	0 to 0	0 to 0	0 to 0	0 to 0	0 to 0	38.5	
2002	262	446	1035	1467	71	32	4	11	1110	1510	167	227	31	0 to 0	0 to 0	0 to 0	0 to 0	0 to 0	0 to 0	0 to 0	0 to 0	38.5	
2003	268	451	1059	1484	71	32	5	12	1135	1528	170	229	26	0 to 0	0 to 0	0 to 0	0 to 0	0 to 0	0 to 0	0 to 0	0 to 0	38.5	
2004	271	448	1071	1474	71	32	6	14	1148	1520	172	228	26	0 to 0	0 to 0	0 to 0	0 to 0	0 to 0	0 to 0	0 to 0	0 to 0	38.5	
2005	301	439	1292	1570	71	32	6	16	1369	1618	205	243	26	0 to 0	0 to 0	0 to 0	0 to 0	0 to 0	0 to 0	0 to 0	0 to 0	38.5	
2006	291	429	1216	1521	72	35	7	18	1295	1574	194	236	10	0 to 0	0 to 0	0 to 0	0 to 0	0 to 0	0 to 0	0 to 0	0 to 0	38.5	
2007	281	423	1170	1499	80	38	7	19	1257	1556	189	233	10	0 to 0	0 to 0	0 to 0	0 to 0	0 to 0	0 to 0	0 to 0	0 to 0	38.5	
2008	288	444	1130	1455	88	45	8	19	1226	1519	184	228	10	0 to 0	0 to 0	0 to 0	0 to 0	0 to 0	0 to 0	0 to 0	0 to 0	38.5	
2009	301	437	1179	1286	107	41	3	24	1289	1351	193	203	10	0 to 0	0 to 0	0 to 0	0 to 0	0 to 0	0 to 0	0 to 0	0 to 0	38.5	
2010	306	442	990	1261	74	52	13	20	1077	1333	162	200	10	0 to 0	0 to 0	0 to 0	0 to 0	0 to 0	0 to 0	0 to 0	0 to 0	38.5	
2011	275	430	1086	1415	82	52	12	19	1180	1486	177	223	10	0 to 0	0 to 0	0 to 0	0 to 0	0 to 0	0 to 0	0 to 0	0 to 0	38.5	
2012	294	443	1161	1457	84	55	10	47	1255	1559	188	234	10	0 to 0	0 to 0	0 to 0	0 to 0	0 to 0	0 to 0	0 to 0	0 to 0	38.5	
Average pumping per $\text{km}^2$		3.95		3.29																			

<sup>a</sup>For years 2000–2004 and 2011–2012, pumping rates are calculated for the respective desert greenery areas from the average of pumping obtained from known data for the years 2005–2010. For 2013 to 2030, the desert greenery area and pumping rate is kept constant in the eastern part as evidenced from the uniform desert greenery area in the recent decades. In the western part, the rate of desert greenery area extension and groundwater pumping has increasing by 3.9%, which is employed as a future prediction in the western part (see Fig. 4)

<sup>b</sup>For years 2000–2004 flow rates are estimated from rate of production

**Fig. 6** Recorded and predicted total groundwater pumping per month for desert greenery activities



is less due to the presence of Sabkha and lesser yield and recharge. Both types of calibration were performed to allow for a quantitative interpretation of the modeling results. The spatial distribution of groundwater levels measured at 68 monitoring wells (Fig. 1) during January 2000 was used for steady state calibration. Time variable data is not involved in this stage of steady state calibration. Spatially distributed initial parameter values for horizontal and vertical hydraulic conductivity, specific yield, and effective porosity were assigned according to available geological information (Fig. 3; Table 3) which are obtained from hundreds of bore holes and pumping tests which are conducted by NDC and USGS during the 1990s regional groundwater research project. All grid elements along the boundaries are assigned spatially variable constant head values (i.e., zero specified flux along the eastern boundary). The heterogeneity and anisotropy may vary differently in real situations based on the geology (Yang et al. 2011). The horizontal and vertical anisotropy directly produce a non-linear decline of groundwater level during the period of groundwater pumping (Ferre and Thomossan 2010). The adjustment of number of parameters may give more accuracy of the developed model (Zhou et al.

2014). Hence, adjustment of aquifer parameters from their initial values was permitted within  $\pm 10\%$ . Several attempts were made and the difference between observed and simulated groundwater levels was minimized by the trial and error method combined with successive aquifer parameter adjustments.

The adjustment of parameters is site-specific to obtain a better match between observed and calibrated groundwater level. In case of anisotropy, the vertical conductivity is usually given a value of one-tenth of the horizontal hydraulic conductivity. In the coastal region, the vertical hydraulic conductivity is calibrated to a maximum of three-tenths of the horizontal hydraulic conductivity due to a very limited horizontal flow than the vertical upward seepage because of the existence of Sabkha. The initial and calibrated aquifer parameters are given in Table 3, while the spatial variation of hydraulic conductivity after calibration is given in Fig. 7. In terms of linear regression between observed and predicted groundwater levels, steady state calibration was achieved with a slope of 1.0, intercept of 0.21 and  $R^2$  of 0.99. The spatial comparison between observed and computed groundwater levels is given in the Fig. 8.

**Table 3** Initial and calibrated aquifer parameters

Layer	Formation	Horizontal hydraulic conductivity (m day <sup>-1</sup> )		Vertical hydraulic conductivity (m day <sup>-1</sup> )		Specific yield	
		Initial	Calibrated	Initial	Calibrated	Initial	Calibrated
1	Sabkhas: carbonates, quartz with minor amounts of feldspar	$2.74 \times 10^{-8}$ to 1.3	$2.74 \times 10^{-8}$ to 1	$2.74 \times 10^{-9}$ to 0.1	$1.37 \times 10^{-8}$ to 0.5	0.01–0.31	0.05–0.32
	Baynunah formation (low productive similar to Sabkhas)	$1.2 \times 10^{-5}$	$1.2 \times 10^{-5}$	$1.2 \times 10^{-6}$	$6 \times 10^{-6}$		
	Sand dunes and gravel and hydrogeologically connected upper fars	0.02–100	0.02–90	0.002–9	0.006–27		
	Weathered outcrop: limestone	12.5–266	10–258	1–25.8	1–25.8		
	Upper fars: conglomerate, dolomitic marls, clay and siltstone	0.8	0.7	0.07	0.07	0.01–0.31	0.01–0.32
2	Lower fars	$5 \times 10^{-2}$	$5 \times 10^{-2}$	$5 \times 10^{-3}$	$5 \times 10^{-3}$	0.1	0.1

**Fig. 7** Spatial variations in horizontal hydraulic conductivity in  $\text{m day}^{-1}$  after calibration (initial value is obtained from USGS 1996)

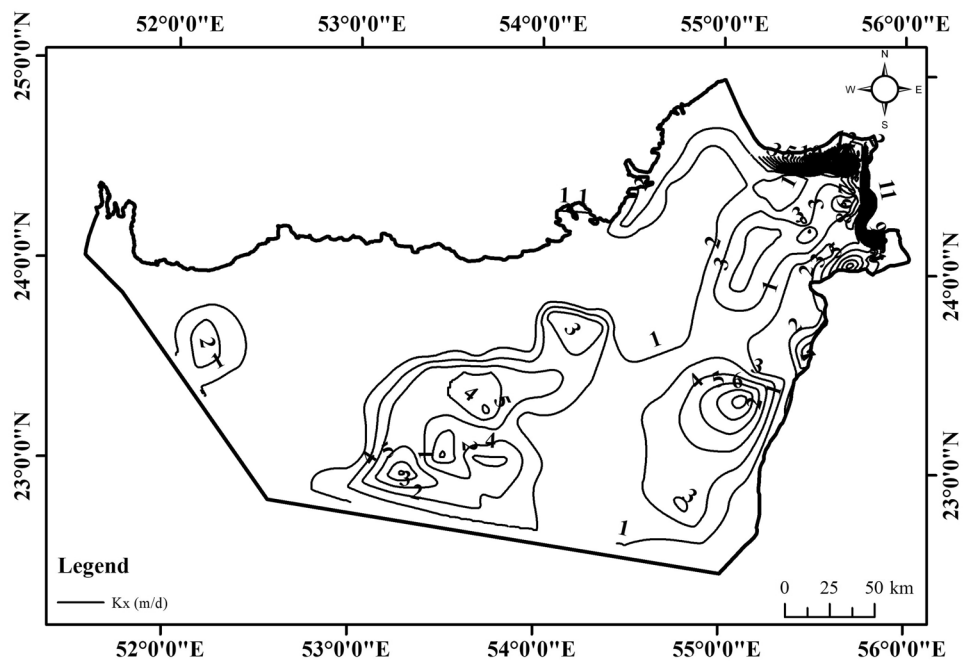
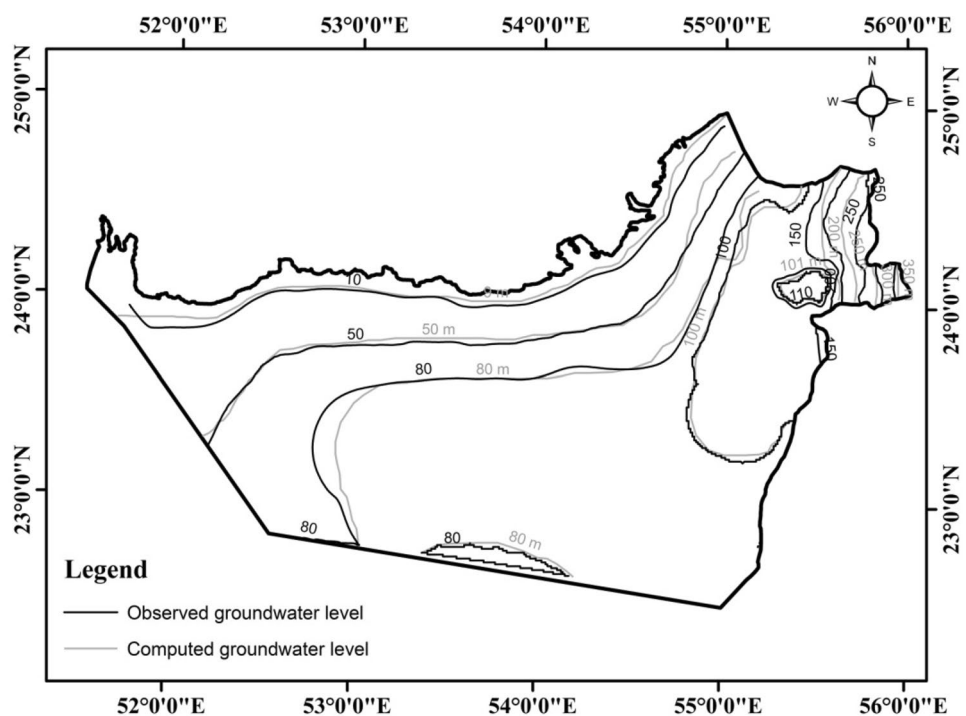


**Fig. 8** Spatial variation of observed and simulated groundwater levels in m above MSL from steady state calibration for January 2000



The model's first 108 monthly stress periods from the year 2000 to 2008 were used for the purpose of transient calibration with all the necessary input variables like possible recharge, discharge and variable boundary settings. The period of simulation used for transient calibration contains the implementation of several water management measures in the study area, which caused localized upwelling of groundwater levels. Simultaneously, groundwater levels

declined in most areas due to the increase of domestic water requirements and the establishment of desert greeneries. The calibrated aquifer parameters, initial head values and time-dependent data, such as monthly prescribed flux across the eastern boundary, monthly seepage of water from the deeper aquifer, prescribed variable head boundary towards the north-east and south-west, and prescribed monthly recharge and monthly discharge were assigned as input parameters.

The dominance of smooth topography and groundwater levels in the model domain, and low conductivity formation along the natural discharge zone (coastal boundary) favor transient model performance with good accuracy. Hence, further trial and error adjustments of model parameters could not improve predictions of transient groundwater levels, and the aquifer parameters that resulting from the steady state calibration were maintained. The wells showing highest difference are located in the eastern part where steep topography exists. The seasonal fluctuation is not major in the study area except the eastern part of the aquifer because of higher recharge from rainfall, Wadi transmission loss and subsurface flow from the Omani Mountains. Both increase and decrease trend in the observed groundwater table was noticed and calibrated in the transient simulation. The best match between the observed and computed groundwater levels is obtained with an  $R^2$  value of 0.99 by comparing a total of 367 data points from 68 monitoring wells distributed throughout the model domain (Fig. 9).

The validation of the model was carried out by comparing observed and computed groundwater levels for a period of 48 stress periods (2009–2012) immediately after the transient calibration. The validation period is fixed on the basis of observed data source from SCAD. The changes in the desert greenery activities and the contribution of water from nonconventional sources were considered during validation (Table 2). Comparison of observed and computed groundwater levels of all the wells during validation and the temporal variation of selected wells are given in Fig. 10. The mean residual between observed and computed groundwater level is 0.27 m during the period of calibration and validation. This value is several times smaller than the mean residual of steady state calibration and confirms the model's ability to produce reliable predictions with notable accuracy.

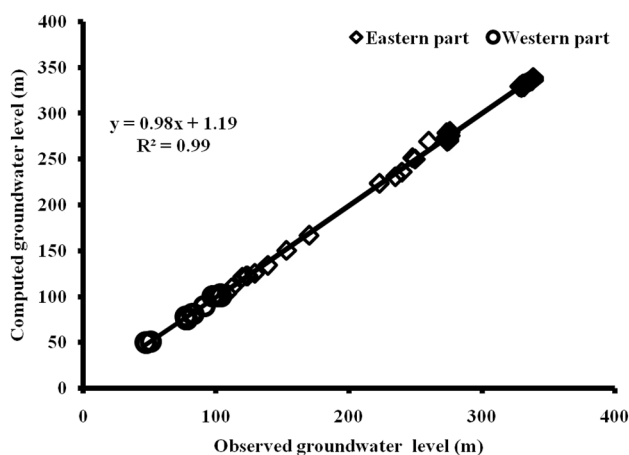
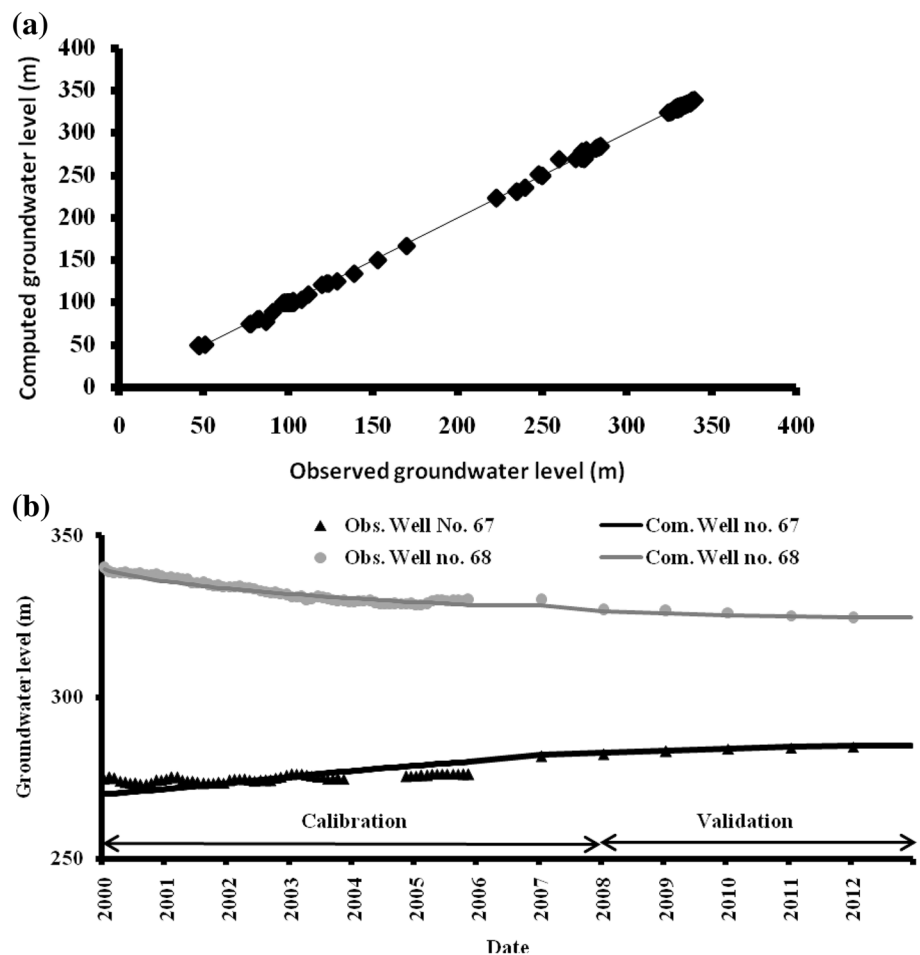


**Fig. 9** Observed and simulated groundwater levels in m above MSL from transient calibration

Apart from seasonal groundwater level fluctuations due to rainfall infiltration recharge, a long-term increase/recovery of groundwater levels was widely noticed during the periods of calibration and validation. This increase of groundwater level was noticed to a maximum of 12.79 m (Well no. 67) in the eastern part and a maximum of 1.2 m (Well no. 12) in the western part. The area near Well no.12 receives groundwater that flows from the sand dunes in the south. In the eastern part, the increase/recovery of groundwater level is noticed due to the reduction in the rate of groundwater pumping in connection with the groundwater management practice in the recent years. The excessive and sporadic upwelling and decline of groundwater level in the eastern part causes a significant variation in the local groundwater flow as well. In the rest of the area, the infiltration of water from the nonconventional sources, which is used for the purpose of greenery activities, considerably counter-balances groundwater pumping and increases groundwater levels at certain locations. A decline in the groundwater level is also observed with a maximum of  $-18$  m in the eastern part and  $-0.35$  m in the western part (sand dunes). This is because of the lack of compensation of nonconventional source of water for the decline of groundwater level and higher pumping of groundwater than recharge. The groundwater level meets the surface in most places of the Sabkha region, because of the low conductivity of the aquifer, which prevents the free discharge of water into the sea. In some areas groundwater seepage is not observed, but an increase in the groundwater level is noticed where the desert greenery activities are occurring. An increase of groundwater level is spotted in Well no. 3 (Fig. 1) due to the irrigation return flow and the contribution of nonconventional water for the greenery activities.

The spatial impact of groundwater pumping varies according to the local characteristics of the aquifer. In the zone of Sabkha, depression cones from pumping are deeper and smaller in diameter due to low hydraulic conductivity. The well field located towards Al Marfa and Al Rahba shows a maximum decline up to  $-20$  m MSL. The spatial extent of groundwater drawdown due to pumping is high in the sand dune areas due to the higher hydraulic conductivity. The location of agriculture well fields is highly sparse and groundwater pumping does not influence one another in the western part. Due to the low hydraulic conductivity, the movement of groundwater into the region of pumping is slow. Hence, the extracted groundwater is derived from the aquifer's local yield capacity resulting in relatively deep groundwater depression cones. In the eastern part, hydraulic conductivity is also predominantly small. However, unlike in the western part, the well fields are located adjacent to each other, such that pumping rates and drawdown affect each other.

**Fig. 10** Validation of simulated groundwater levels from 2009 to 2012 (a) and temporal variation of groundwater levels from 2000 to 2012 for wells 67 and 68 (b)



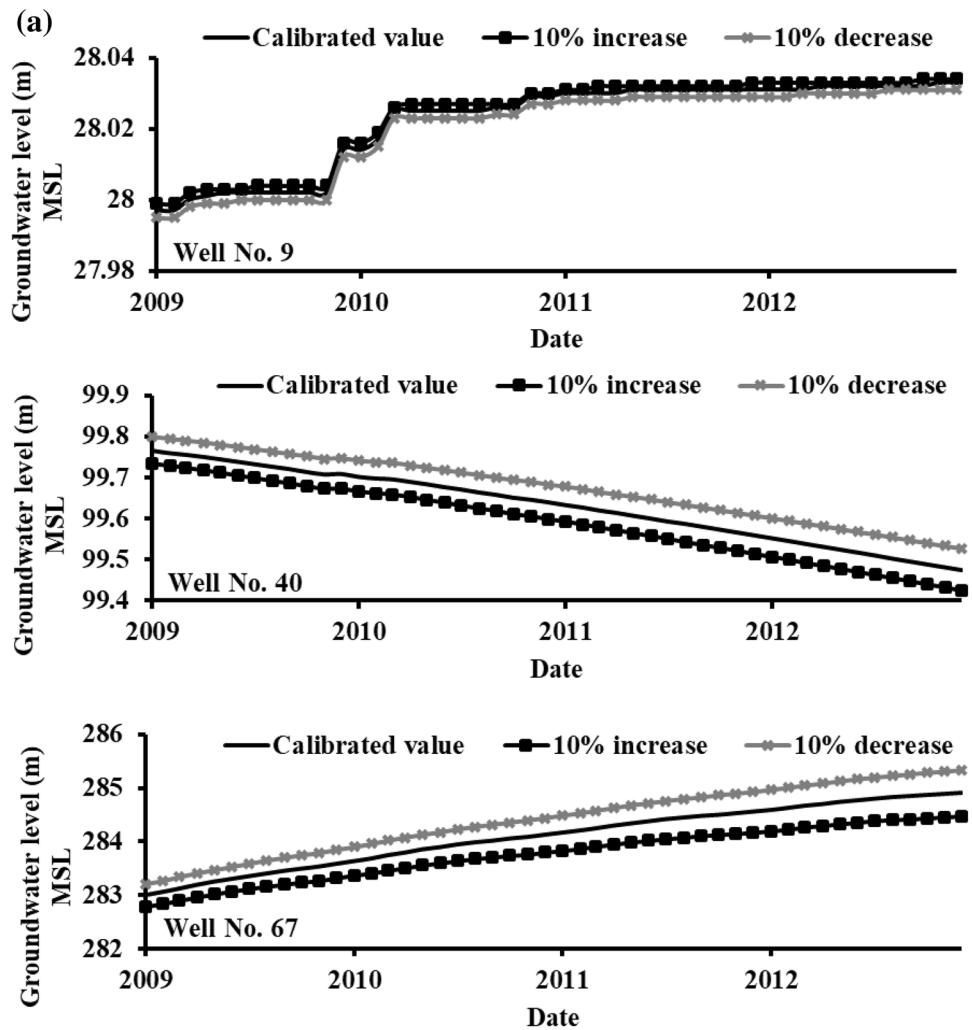
**Sensitivity analysis**

The uncertainty in the aquifer parameters can be understood by sensitivity analysis. Aquifer parameters used in the model were obtained from more than 100 locations. Still, the sensitivity analysis is conducted to understand the uncertainty in the model performance. This analysis will also help to understand the data gap and influence of various parameters to simulated groundwater level (Anderson et al. 2015; Hill and Tiedeman 2006). The input parameters such as hydraulic conductivity and specific yield were assessed by an increase and a decrease of 10%. The sensitivity of the model is shown in Fig. 11.

These wells are shown from each geomorphic unit representing the sensitivity of the particular well’s location in the geomorphic zone. It does not represent the behavior of the entire geomorphic zone. Few wells are showing decline and others are showing an increase in the groundwater level based on site-specific hydrogeologic stresses. The well 40 is for dune surface, 67 is for gravel plain, and 9 is for coastal area (without sabkha formation). The grid size of the developed model is fixed as 3 km<sup>2</sup> to avoid computational error. The location of the

observation wells may not be at the center of each grid. To analyse the sensitivity of the model to grid size, the grid refinement to 500 m is applied for each location of the representative observation wells and nil changes are noticed in the simulated groundwater level. The changes in the horizontal hydraulic conductivity produced  $\pm 0.43$  m change in the simulated groundwater level at the eastern area (well no. 67),  $\pm 0.05$  m at dune surface (well no. 40), and 0.002 m (well no. 9) at the north western coastal part. There are nil changes in the simulated groundwater level associated with a change in the vertical hydraulic conductivity by  $\pm 10\%$ . The groundwater level is varied between  $-0.55$  and  $0.64$  m when changing specific yield by  $\pm 10\%$ . The changes are  $\pm 0.1$ ,  $\pm 0.02$  m and between  $-0.55$  and  $0.64$  m at dune surface, coastal part and eastern part, respectively. Comparison of the sensitivity results show that the changes in the groundwater level were most sensitive to changes in the specific yield than horizontal conductivity. The nil sensitiveness of groundwater level to changes in vertical conductivity is because of universal rule that aquifer system is dominated by horizontal flow under the condition of saturation. However, the changes in the groundwater level obtained by sensitivity analysis

**Fig. 11** **a** Sensitivity of the model to  $\pm 10\%$  change in aquifer parameter (horizontal hydraulic conductivity). **b** Sensitivity of the model to  $\pm 10\%$  change in aquifer parameter (vertical hydraulic conductivity). **c** Sensitivity of the model to  $\pm 10\%$  change in aquifer parameter (specific yield)



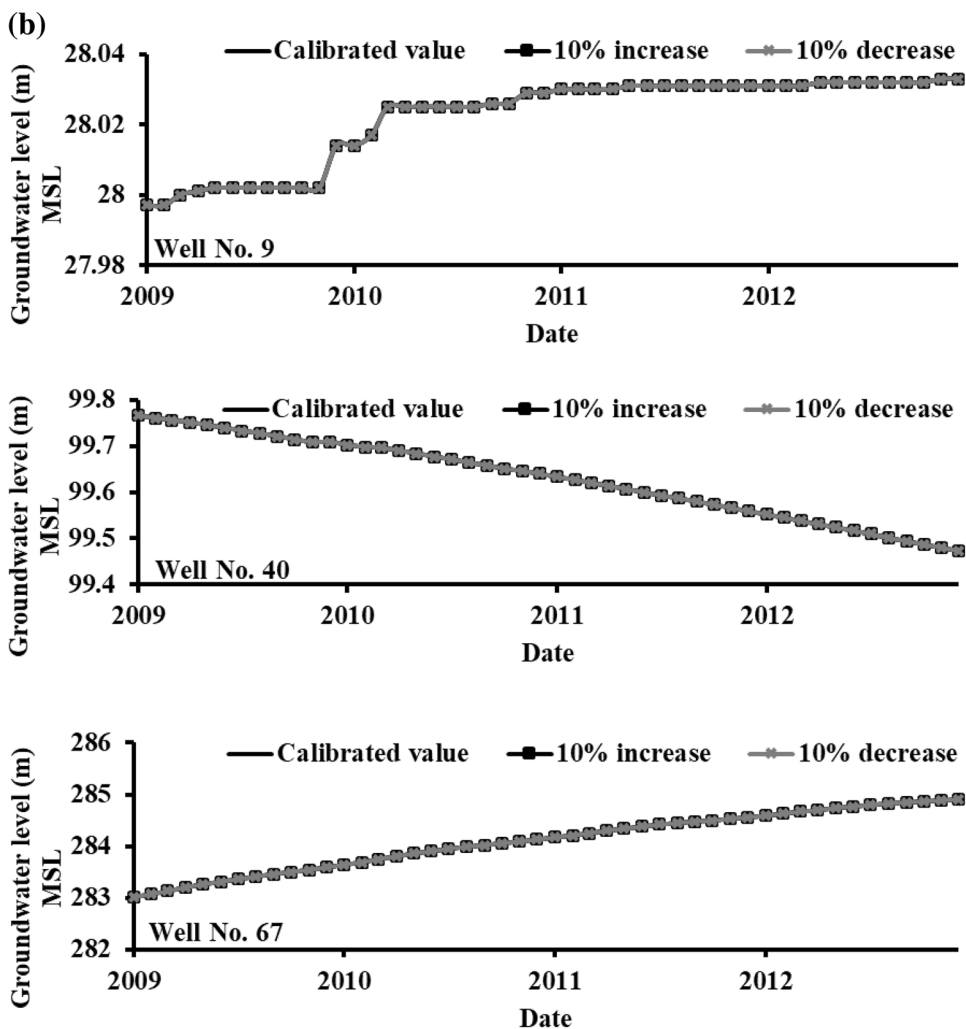
were not much significant indicating that the model can be used further to predict the scenarios.

## Business as usual predictions

For long-term groundwater management in the presence of pumping and infiltration from nonconventional sources, it is essential to control excessive declines and upwelling of local groundwater levels. While continuously declining groundwater levels indicate aquifer depletion, groundwater level depths within 5 m below ground surface may be detrimental for building foundations. To investigate future perspectives, the model was run to year 2030 using present (2012) level of recharge and groundwater pumping according to Fig. 6. The temporal variations of predicted groundwater levels up to 2030 are shown in Fig. 12. The predicted changes in the groundwater levels in the sand dune area occur between  $-2$  m (well no. 41) and  $1.68$  m, (well no. 12). In the eastern part, an increase of  $5.57$  m in groundwater level is noticed in

well no. 65. A decline of groundwater level up to  $-5.08$  m is observed in wells no. 61, 62 and 63, which are located in one of the important agricultural fields named Al Hayer. Similarly, in well no. 68 at Zarob, a groundwater level decline is predicted up to  $-3.9$  m. The predicted fluctuations of groundwater levels for all wells are given in Fig. 13. The spatial comparison of groundwater level contours between the years 2012 and 2030 is prepared by grid wise investigation (Fig. 14). Most of the wells in the sand dune area show a slight decline in groundwater level. However, the areal extend of groundwater decline is limited and regional comparison presume that the groundwater level in sand dune area remains unchanged. Towards southern boundary and at the northern fringes of dune area, the decline of groundwater level occurs in between the range of  $-4$  and  $-1$  m. In the eastern part, other than the location of observation wells, the increase of  $15$  m and decline of  $-10$  m is noticed in the groundwater level. The increase of groundwater level at various magnitudes confirms the recovery of groundwater level. The increased use of nonconventional

Fig. 11 (continued)

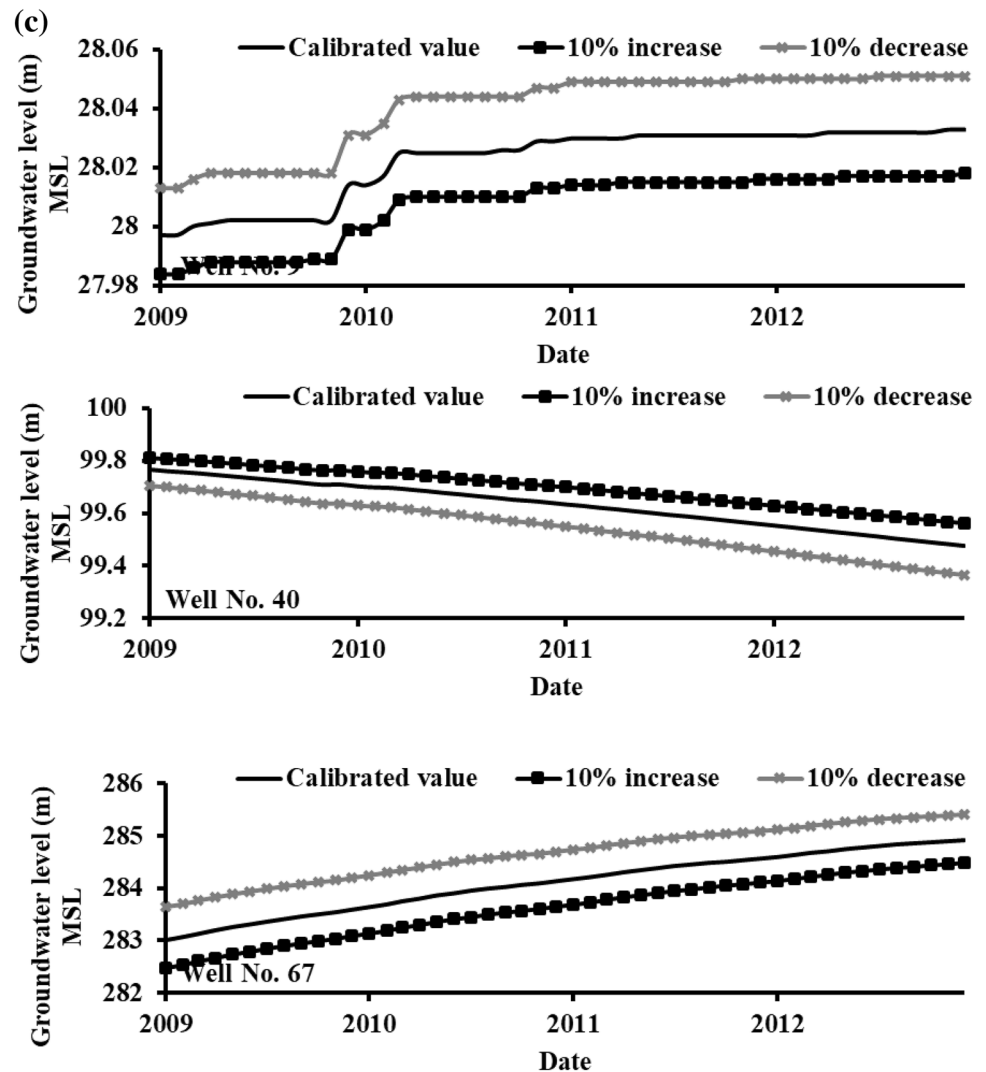


water sources, the reduction in groundwater pumping, and the irrigation return flow into groundwater can all be reasons for the increase in groundwater level. The decline is at the location of desert greenery activities towards extreme east and north-east represents the pumping is still heavy. Overall, in the eastern part, the increase and decrease of groundwater level is noticed and in the western part, the groundwater level is unchanged in the sand dune area. Even there is a decline, it is not at the regional scale. The maximum decrease of groundwater level of  $-4$  m was noticed at the southern boundary. In the dune surface, the maximum of 2 m decrease is noticed in well no. 41. Towards north eastern coastal boundary, the increase of groundwater level is also noticed with a maximum of 2 m. The increase and decrease of groundwater level are observed without significant impact on the regional groundwater flow.

The zone of seepage is identified along the coast, western part and south-eastern part. The previous two regions are geologically occupied by Sabkha. The predicted upwelling of groundwater level for wells no. 1

and 2 located in the Sabkha region is consistent with the independent study by Stanford and Wood (2001). In the remaining areas, an increase of groundwater level to the ground surface is noted in observation wells no. 1, 2, 46 and 48. The maximum occurs at well no. 48, where a reduction in pumping and its location in the downstream of drainage area Dank that receives a large quantity of subsurface flow lead to efficient recovery of groundwater levels. The groundwater level is predicted to reach the ground surface in October 2022. The aquifer is already a subject of low conductive formation. The presence of mound-shaped groundwater level in the dune surfaces prevents regional westward flow of groundwater and results in further reduction in the flow of groundwater in the low conductive aquifer. The significant subsurface inflow along the drainage Dank and presence of mound-shaped groundwater level in the dune surface supports the fast recovery of groundwater level that forms zone of seepage towards south-west.

Fig. 11 (continued)



## Future scenarios

The recent increase in the dependency on nonconventional sources induces prolonged alterations in the aquifer stress. The spread of desert greenery in a hyper-arid climatic condition is challenging but a viable task given the availability of nonconventional water sources. On the other hand, investment of money for production of water is several times higher than the agricultural production. Hence, in the near future, changes in greenery activities may occur intentionally and the pumping of groundwater can be either reduced or increased depending on the water demand. Rainfall and drainage transmission loss are highly susceptible to changes. Hence, other than above anthropogenic influenced stresses, irregular or limited natural aquifer replenishment might also be a major unavoidable threat. The rainfall recharge in Abu Dhabi is considerably less than the recharge caused by subsurface lateral flow and drainage transmission loss from Oman Mountain. It

seems Oman Mountain recharge is very important, but uncertainly, the rainfall is not uniform and expected to change in the future from  $-20$  to  $+10\%$  in 2050 (MoE 2006). This may either reduce or increase the quantity of rainfall recharge and drainage transmission loss. Hence, the developed groundwater model was used to study the impact of the changes in aquifer stress induced by natural and anthropogenic factors by changing the pumping of groundwater for greenery and domestic activities, by changing rainfall recharge, and by changing rainfall and drainage transmission loss from Oman Mountain. A total of 24 scenarios were analyzed using different assumptions in each category consisting of sudden (January 2013) step changes of  $\pm 5$ ,  $\pm 10$ ,  $\pm 20\%$ . The maximum impact of  $\pm 20\%$  change in each category is discussed in detail here. Results for  $\pm 5$  and  $\pm 10\%$  are similar in nature but weaker in magnitude. Figure 15 shows the predicted regional change in groundwater level by the model under scenarios of  $\pm 20\%$  in each category.



**Fig. 12** Predicted groundwater levels for selected well at sand dune (a) and eastern part (b) from 2013 to 2030 with present levels of recharge and discharge

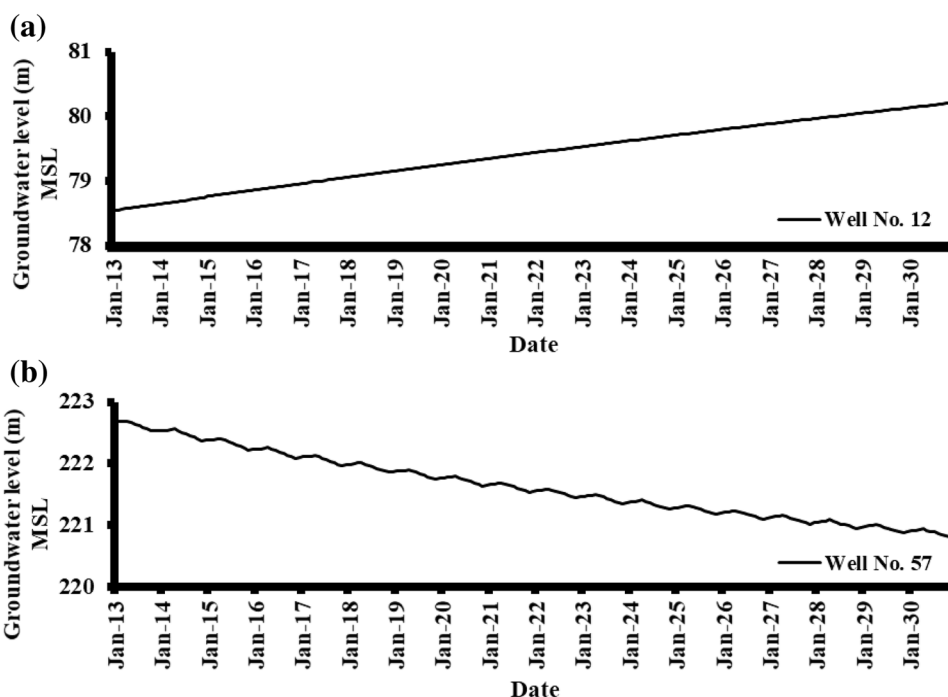
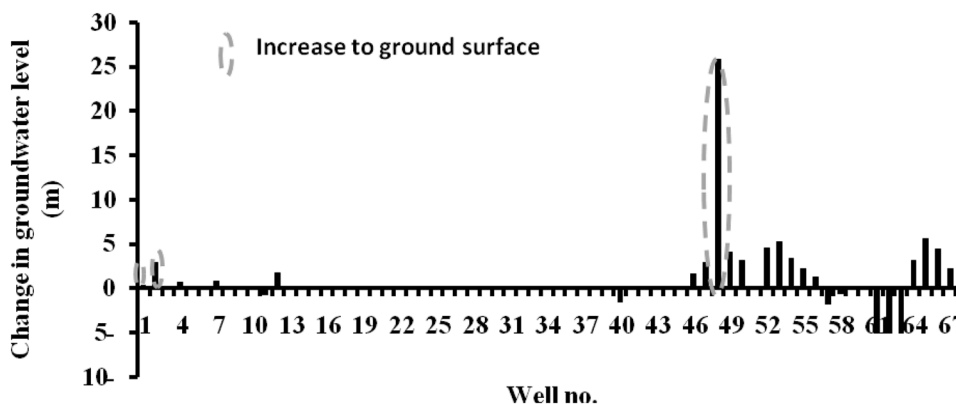


**Fig. 13** Change in groundwater level from 2013 to 2030



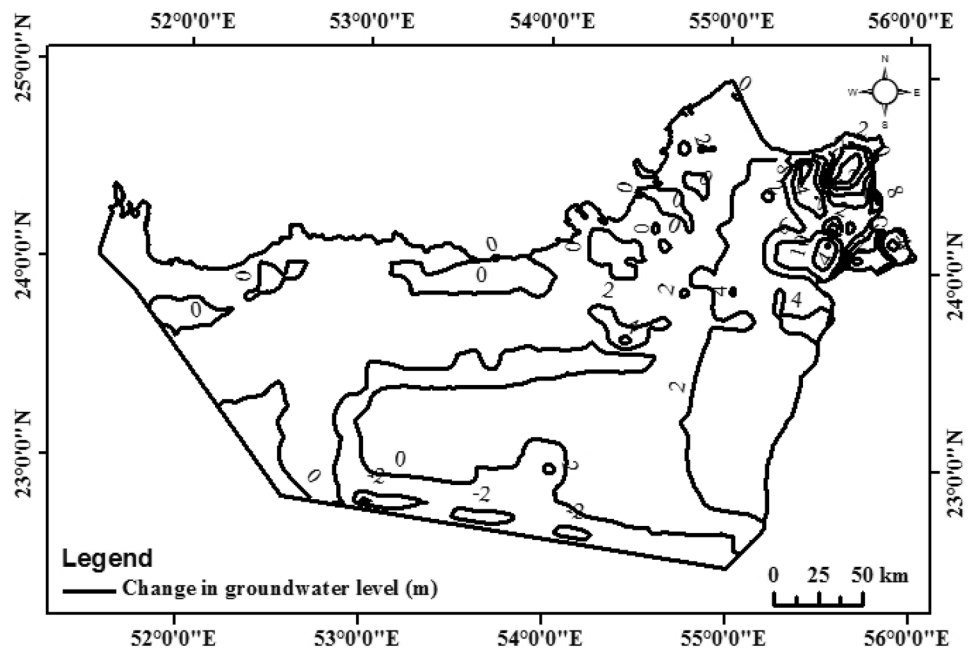
**Alterations in desert greenery area and domestic pumping**

Both reducing and increasing the greenery area are possible alternatives and, thus, considered here. A increase of 20% in greenery (Fig. 15a) will decrease the groundwater level by a maximum of  $-5.6$  m in wells 61,62 and 63 located in the north eastern corner of the study area (Al Hayer).The decline is comparatively higher than the decline predicted using present level greenery pumping. Also, the increase of groundwater level in this scenario is noticed by a maximum of 4.98 m in well no. 65 which is also comparatively less than the recovery predicted using present level greenery pumping. A 20% decrease in greenery (Fig. 15b) will increase the groundwater level by a maximum of 6.19 m in well no. 65 located in the

eastern corner of the study area. The maximum decrease of groundwater level of  $-4.87$  m is noticed in the same wells at Al Hayer. Over all, the regional recovery of groundwater level in the eastern part occurs at a maximum of 15 m which is not affected by changes in greenery activities up to  $\pm 20\%$ .

At selective location (Al Sarooj), the increase of desert greenery area also controls groundwater decline. The predicted decline in the eastern part (Al Sarooj) is  $-4.5$  m which is nearly half of the decline predicted with present level desert greenery pumping. The investigation under changes in desert greenery area shows that both the maximum and minimum changes in the groundwater level are noticed in the eastern part of the area due to the contribution of water from nonconventional source and the influence of heavy pumping for desert greenery activities.

**Fig. 14** Change in groundwater levels between December 2012 and December 2030



Towards western part, the regional changes in the groundwater level are less significant. Groundwater levels in many of the observation wells located in the sand dune area insensitive to desert greenery activity showing a rise of 0.2 m for all pumping scenarios. The increase of greenery pumping reduces groundwater levels at only local scale. In the sand dune area, the decrease of groundwater level reached a maximum of  $-2$  m, in well no. 40 during an increase of 20% of greenery activities. In contrast, the decrease in groundwater level was only  $-1.41$  m in the same well for a 20% decrease of greenery activities. The predicted temporal groundwater level for selective wells under various scenarios is given in Fig. 16. Few wells are sensitive only to the changes in desert greenery and few wells are sensitive only to changes in rainfall and drainage transmission loss. In other words, this means that the extreme pumping of groundwater from well fields will not influence the wells located at the regional level, unless pumping extends over long periods.

Under the scenario of both increase and decrease of 20% of greenery activities, the wells located in the Sabkha (wells no. 1 and 2) show the groundwater level is above the ground surface. It will produce a zone of discharge of groundwater by means of evaporation. The groundwater level in wells no. 46 and 48 located at the downstream of drainage Dank reaches the ground surface. Well no. 3, 32, 37 and 47 will have groundwater level within 5 m below ground surface. The changes in groundwater levels during various scenarios at the observation wells are given in Table 4.

A continuous decrease in groundwater level was also noticed in many wells, for example, well no. 57 (Fig. 16b) located in the agriculture well fields at the north eastern boundary. In both increased and decreased pumping

scenarios, increase in groundwater levels is not observed. This decline of groundwater level even under the reduced desert greenery activities confirms existence of heavy exploitation of groundwater in this part. This recommends either a need of additional contribution of nonconventional water sources for existing desert greeneries or cropping less water consuming plants or further reduction in the area of greenery.

The limited volume of domestic pumping is applicable only in the eastern part. The rate of domestic pumping is already reduced to  $10 \times 10^6 \text{ m}^3 \text{ year}^{-1}$ . The change in the rate of domestic pumping by  $\pm 20\%$  represents least impact that changes groundwater level of  $\pm 0.1$  m only in the eastern part. In the western region, there is no pumping of groundwater for domestic purpose and the impact of change in domestic pumping is also nil.

### Variations in rainfall and drainage transmission loss

Out of the four categories (change in area of greenery, change in rainfall recharge, change in rainfall and drainage transmission loss and change in domestic pumping), rainfall and drainage transmission loss have higher possibilities to undergo changes in the future. Change in rainfall might cause changes in runoff that will modify the quantity of drainage transmission loss across eastern boundary. But, lateral subsurface recharge might always be present. When rainfall fails or is less than the quantity enough to produce runoff, this scenario is applicable. In this scenario, recharge by means of subsurface lateral flow is always present across the eastern boundary and changes may occur in the volume of rainfall. Groundwater level, even along

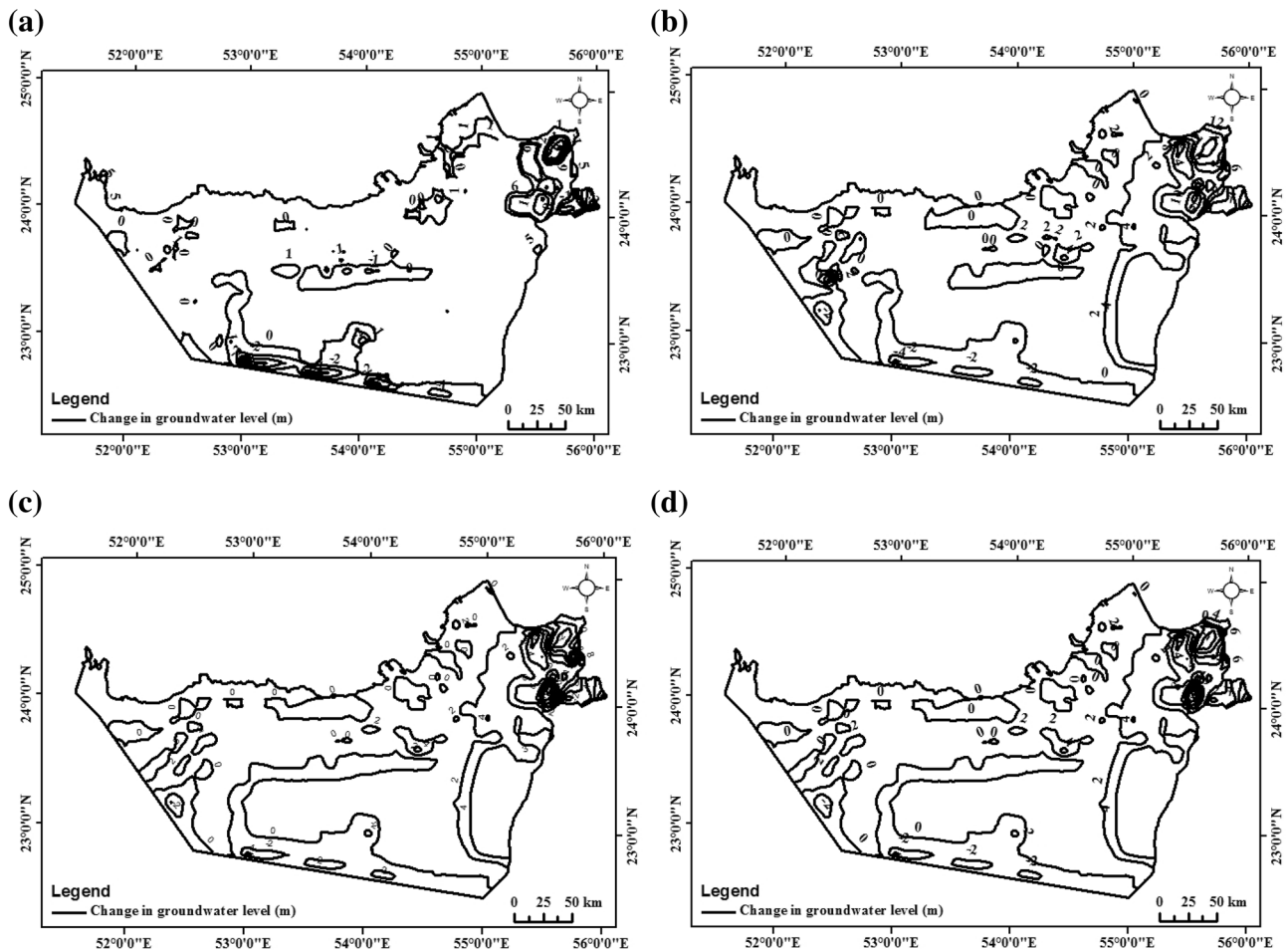


**Fig. 15** **a** Predicted change in regional groundwater level from December 2012 to December 2030 (20% increase in desert greenery groundwater pumping). **b** Predicted change in regional groundwater level from December 2012 to December 2030 (20% decrease in desert greenery groundwater pumping). **c** Predicted change in regional groundwater level from December 2012 to December 2030 (20% increase in domestic groundwater pumping). **d** Predicted change in regional groundwater level from December 2012 to December 2030 (20% decrease in domestic groundwater pumping). **e**

Predicted change in regional groundwater level from December 2012 to December 2030 (20% increase in rainfall recharge and runoff). **f** Predicted change in regional groundwater level from December 2012 to December 2030 (20% decrease in rainfall recharge and runoff). **g** Predicted change in regional groundwater level from December 2012 to December 2030 (20% increase in rainfall recharge). **h** Predicted change in regional groundwater level from December 2012 to December 2030 (20% decrease in rainfall recharge)

the boundary, is affected in response to a change of  $\pm 20\%$ . The impact is noted especially in the eastern part. Neither decrease nor increase in the transmission loss will affect the groundwater level in the western part. However, site-specific isolated increase in the groundwater level is noticed. It also permits the formation of zone of seepage in the south east. The results obtained from the model with these scenarios show that an increase of 20% in the rainfall will increase the groundwater level by 7.5 m in the eastern part of the study area. The 20% increase of drainage transmission loss results in maximum increase of 2.3 m along boundary that is responsible for regional increase of groundwater level by maximum of 1.7 m. The maximum recovery of groundwater level obtained by grid wise investigation is 16 m (Fig. 15e).

Similarly, the 20% decline in the transmission loss will reduce the groundwater level by maximum of 2.5 in which the groundwater level is regionally reduced by maximum of 2.7 m.

Cloud seeding and geographical impact in the intensity of rainfall may result in change of rainfall only in Abu Dhabi without change in the rainfall at Oman Mountain. Hence, rainfall without affecting drainage transmission loss across the eastern boundary is also possible. In this scenario, subsurface lateral flow and drainage transmission loss is always present and changes occur only in the volume of rainfall. The model shows an increase in groundwater level by 5.69 m in the eastern zone when the rainfall is increased by 20%. An increase of groundwater level is also noticed by 5.49 m even

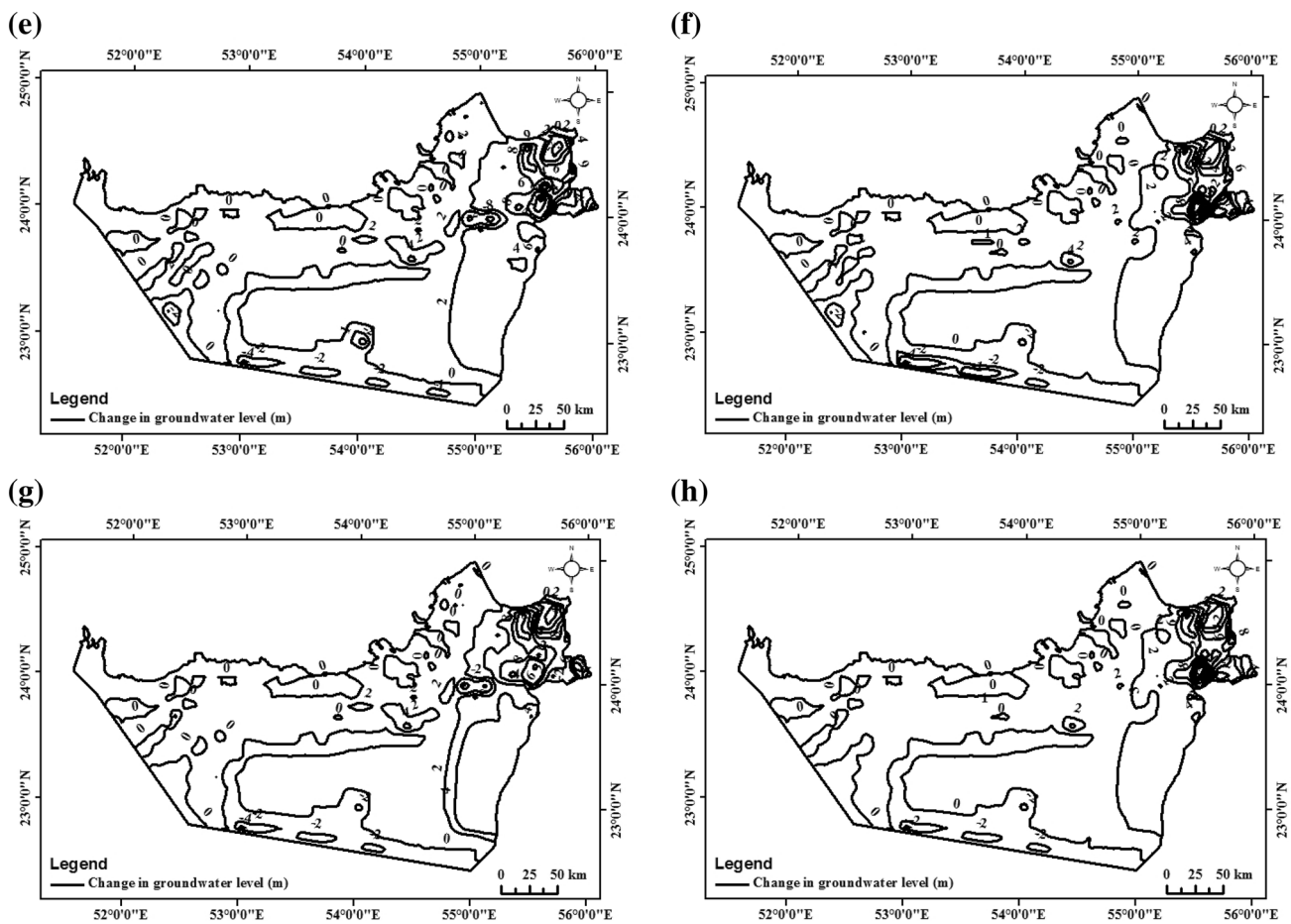


Fig. 15 (continued)

when decreasing rainfall by 20%. The decline of groundwater level under the investigation by increase and decrease of 20% rainfall is predicted as  $-4.91$  and  $-5.11$  m respectively.

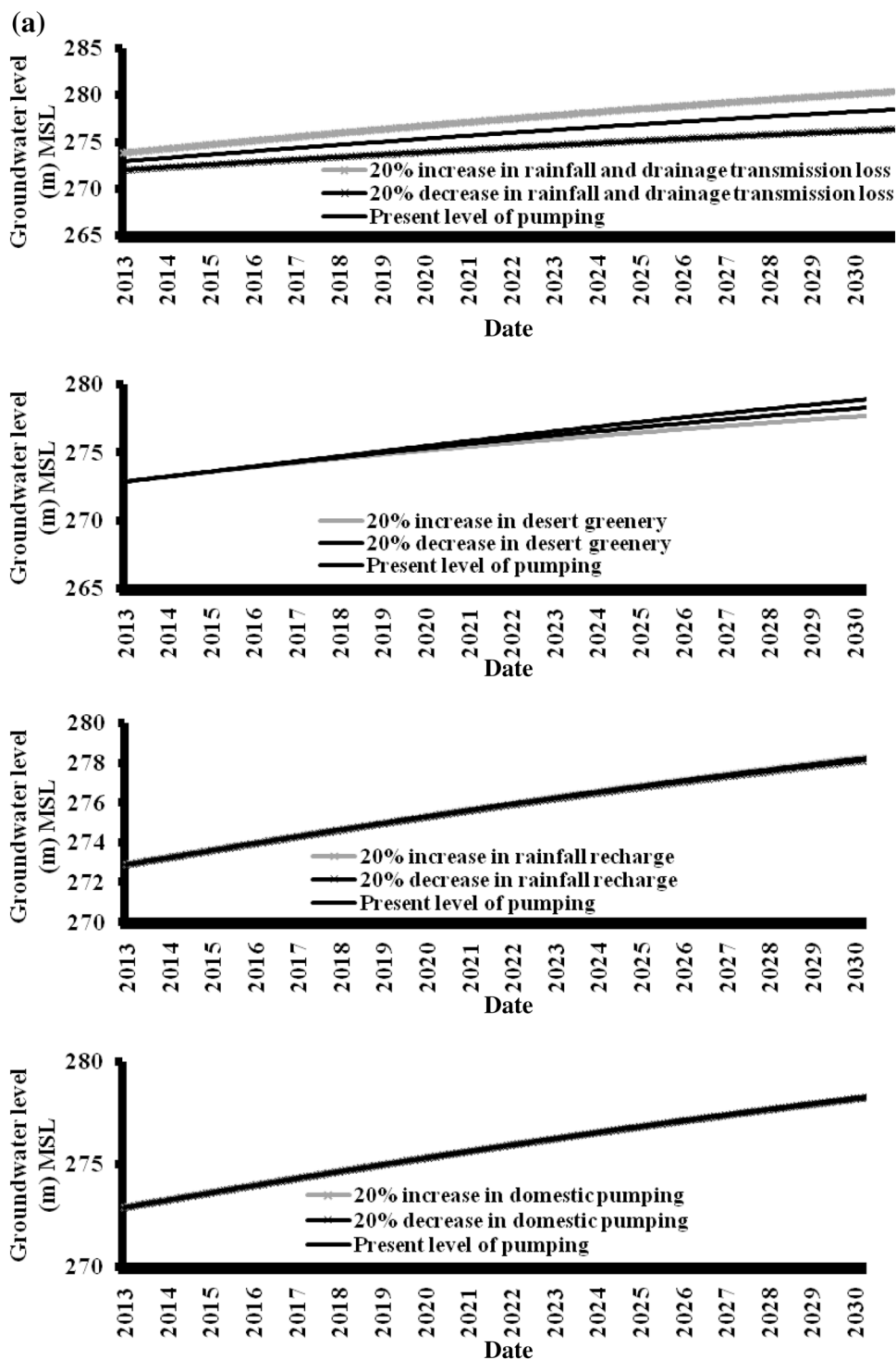
By comparing results of different scenarios, it is understood that the fluctuation of groundwater is comparatively irregular, high and regionally connected impact is noticed in the eastern part of the Abu Dhabi. The impact of increased and decreased pumping is highly sporadic and not at regional level in the western part. Groundwater seepage to the land surface commonly happens along the region of coastal Sabkha and south east. The decrease of groundwater level is noticed at local level due to isolated cone of depression. Similarly, at some locations especially in the eastern part, a decrease of groundwater levels is predicted even under the scenario of reduced pumping. This confirms that the groundwater resource is under threat and a need of additional contribution of non-conventional water or reduction in the groundwater-based greenery activities. In the eastern parts, the upwelling of groundwater level was also noticed even under the scenario of reduced recharge, drainage transmission loss and pumping in some places which prove the

gradual recovery of groundwater level. These situations can be managed by monitoring of site-specific nonconventional water contribution based on local hydrogeological condition. Among the predicted fluctuations, the western part is more sensitive to the use of nonconventional water source and the eastern part is sensitive to the use of nonconventional water source, change of recharge along eastern boundary and rainfall. Among the predicted increase and decrease of groundwater level, no significant change occurs in the overall regional flow patterns.

## Summary and conclusions

The Abu Dhabi aquifer is known to suffer from hydrological stress, both quality and quantity wise. To provide a useful quantitative freshwater resources management tool, the present study develops a regional groundwater model for the Abu Dhabi Emirate. The model is constructed in MODFLOW (finite differences) and based on topographic and geological information. Using recorded groundwater level

**Fig. 16** **a** Predicted groundwater level under various scenarios in well no. 65. **b** Predicted groundwater level under various scenarios in well no. 57. **c** Predicted groundwater level under various scenarios in well no. 40

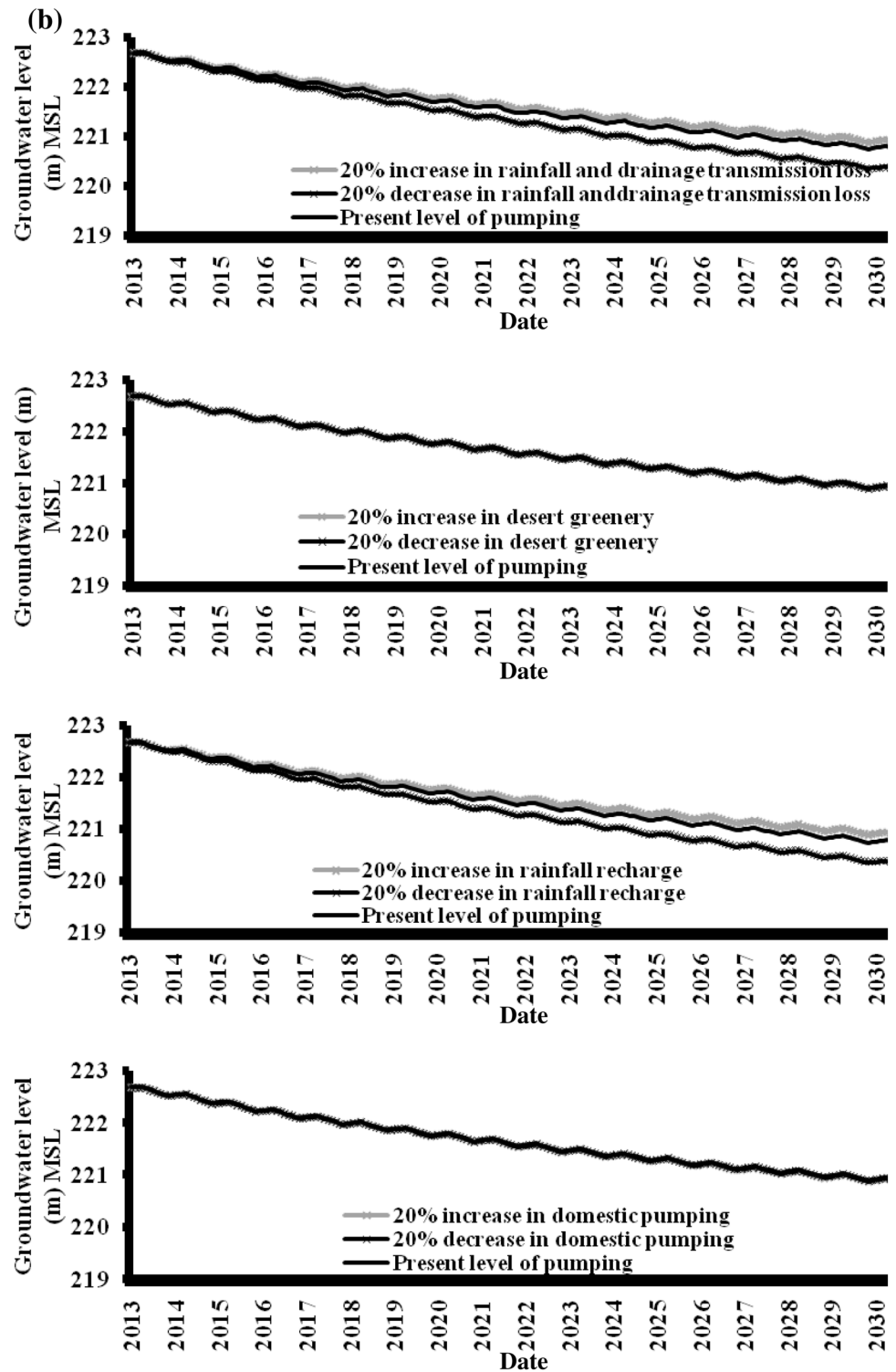


data over more than one decade, steady state and transient calibration steps were performed with the mean residual value of 0.27 m falling within the range of acceptance, followed by successful model validation. The major hydrological drivers considered by the model are recharge due to rainfall, freshwater production from nonconventional sources, subsurface inflow and drainage transmission loss from the

Oman Mountains and discharge due to pumping for greenery and domestic purposes. Results are presented in terms of changes in groundwater levels and potential for excessive lowering (depletion) and excessive rising (upwelling).

The pumping of groundwater is mainly for the purpose of greenery activities and limited amount to domestic purpose applicable only in the eastern part. The spatial distribution

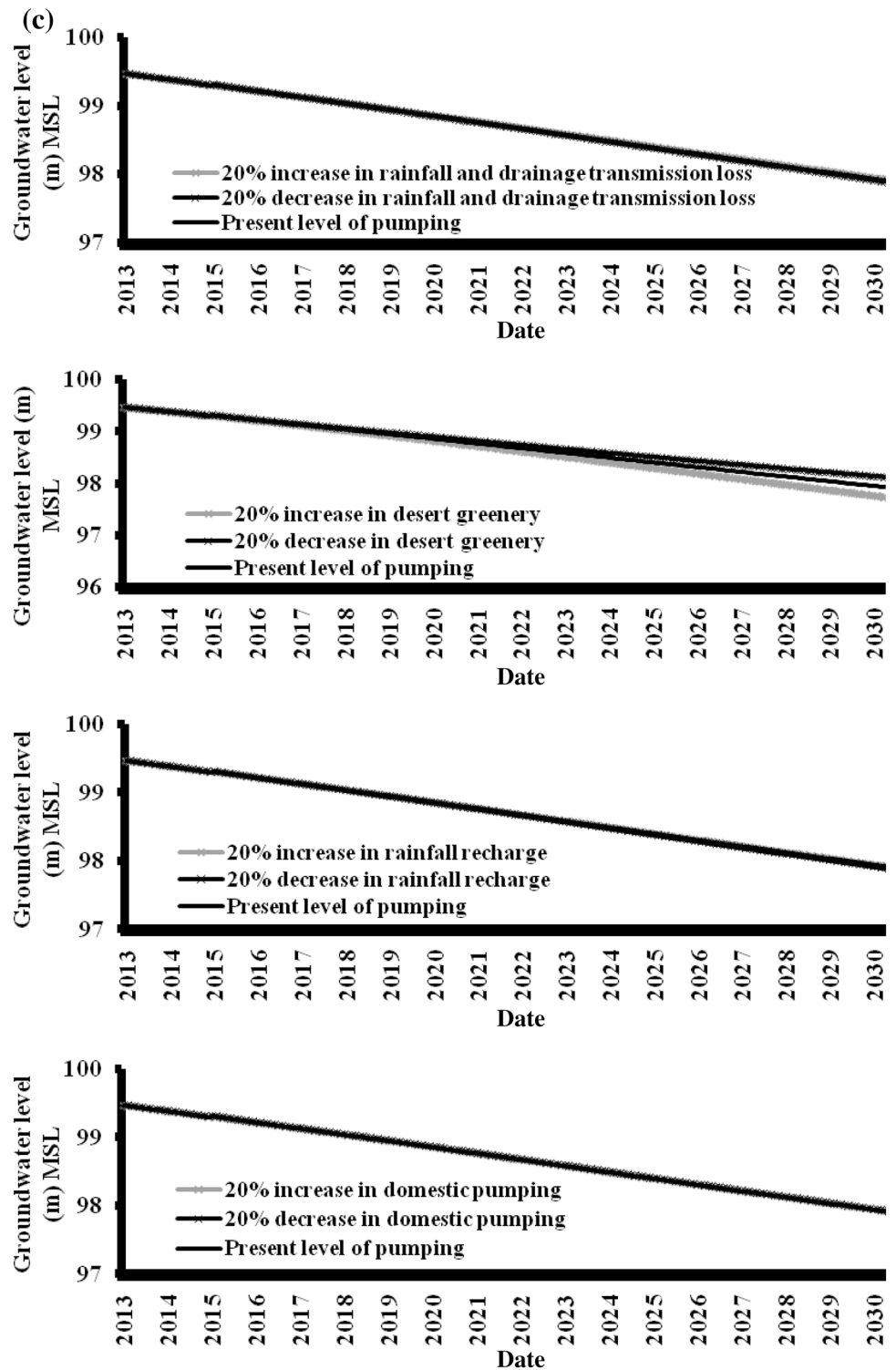
Fig. 16 (continued)



of desert greenery is relatively uniform in the eastern part and increasing at the rate of 3.9% on average towards western part. For each square kilometer of the greenery areas, the average groundwater pumping of  $3.29 \times 10^6 \text{ m}^3 \text{ year}^{-1}$  in the eastern part and  $3.95 \times 10^6 \text{ m}^3 \text{ year}^{-1}$  in the western part were estimated and used for the model development.

During the calibration and validation stage, a mean residual of 0.27 m is noticed between observed and computed groundwater level. An increase of groundwater level to a maximum of 12.79 m (well no. 67) in the eastern part and 1.2 m in the area of sand dune area is calibrated and validated in this stage. Due to limited contribution from

Fig. 16 (continued)



nonconventional sources of water in the greenery activities, a decline in the groundwater level is also observed with a maximum of  $-18$  m in the eastern part and  $-0.35$  m in the sand dune area.

Understanding the groundwater system and its response is an essential element for the sustainable development of

groundwater resource strategies for the future. Hence, the model was run for a period up to 2030 with the present level of pumping. It is predicted/identified that the eastern part is more sensitive to recharge than the western part. Consistent with previous studies by various authors, both rainfall and the portion of water derived from Oman Mountain

**Table 4** Change in groundwater level (m) for various scenarios (observation wells)

Scenarios	Overall area		Sand dune		North eastern		Eastern side		Groundwater level reaching ground surface Well no.
	Maximum increase	Maximum decline	Maximum incline	Maximum decline	Maximum incline	Maximum decline	Maximum incline	Maximum decline	
Desert greenery activities									
–20%	6.19	–4.87	1.68 (well no. 12)	–1.41 (well no. 40)	0.19	NA	6.19	–4.87	Well no. 1, 3, 46 and 48
+20%	4.98	–5.6	1.57 (well no. 12)	–2 (well no. 40)	0.19	NA	4.98	–5.6	Well no. 1, 3, 46 and 48
Change in domestic water pumping									
–20%	5.59	–4.95	0.21	–1.61	0.19	NA	5.59	–4.95	Well no. 1, 3, 46 and 48
+20%	5.55	–5.2	0.21	–1.61	0.19	NA	5.55	–5.2	Well no. 1, 3, 46 and 48
Change in rainfall recharge + drainage transmission loss									
–20%	6.23	–11.2	0.11	–1.64	0.16	NA	3.47	–11.2	Well no. 1, 3, 46 and 48
+20%	7.5	–3.51	0.11	–1.32	0.25	NA	7.5	–3.51	Well no. 1, 3, 46 and 48
Change in rainfall recharge									
–20%	5.45	–5.11	0.11	–1.64	0.16	NA	5.45	–5.11	Well no. 1, 3, 46 and 48
+20%	5.69	–4.91	0.65	–1.58	0.25	NA	5.69	–4.91	Well no. 1, 3, 46 and 48

contributing to groundwater recharge are estimated to be larger in the eastern part of the Emirate. In the eastern part, of groundwater level is noticed with a 15 m of increase to –10 m of decrease. The wells in the western part show differences of –2 to 1.68 m in the groundwater level. The groundwater level depression due to pumping remains localized. Low hydraulic conductivity formations in the western part induced localized depression cones during groundwater extraction. In the eastern part, on the other hand, cones of depressions are overlapped because wells are closer to each other.

In most greenery well fields, declines of groundwater level are limited because of the contribution of nonconventional water. In the sand dune area, the decline of groundwater level under present level of pumping is noticed which needs more contribution of non-conventional water. The observation wells located outside the greenery areas represent increases in groundwater levels. The limited decline of groundwater in the eastern part indicates recovery of groundwater level due to reduced groundwater pumping and increased recharge from non-conventional sources. The increase of groundwater level to a depth of 5 m below the ground surface may create a risk to the foundations of buildings. In the well numbers 1, 2, 46 and 48, an increase of groundwater level to the ground surface is noticed. A

remarkable groundwater level change is recorded in the well located in the downstream of drainage Dank, where groundwater level will reach ground surface in October 2022.

The developed model was also used to analyze 24 scenarios considering change in groundwater pumping rates for greenery activities, domestic pumping, change in recharge and change in rainfall and drainage transmission loss off from Oman Mountain. The maximum impact of  $\pm 20\%$  change in each category is explicitly discussed. Among the four categories, rainfall and drainage transmission loss have the highest possibilities to undergo changes. Extreme changes of groundwater levels are observed at isolated locations without significant impact on the regional groundwater flow pattern. A decrease in groundwater level was noticed in few places under different scenarios even with reduced pumping indicating the groundwater resource is under threat and contribution of more non-conventional water resources might alleviate the problem. The observed upwelling of groundwater in the eastern part even after intense pumping shows the gradual recovery/increase of groundwater level in this region. Since the use of non-conventional water resource is increased especially for the purpose of existing desert greenery and for the development of new desert greenery, care must be taken to avoid unexpected increase in the groundwater level as close as to ground surface. This



model can be employed as the main tool in groundwater management in the Emirate of Abu Dhabi. It can serve as a main component in several decision support systems that seek management decisions related to groundwater quantity and quality in the future.

**Acknowledgements** The authors would like to express their sincere appreciation to the National Water Center, UAE and the United Arab Emirates University for the financial support of this project under Grant number 31R112.

## References

- Abdulaziz AM, Faid A (2015) Evaluation of the groundwater resources potential of Siwa Oasis using three dimensional multilayer groundwater flow model, Mersa Matruh Governorate, Egypt. *Arab J Geosci* 8(2):659–675
- Al Dhaheri S, Saji A (2013) Water quality and brine shrimp (*Artemia* sp.) population in Al Wathba Lake, Al Wathba Wetland Reserve, Abu Dhabi Emirate, UAE. *Int J Biodivers Conserv* 5(5):281–288. <https://doi.org/10.5897/IJBC12.056>
- Al Shahi FA (2002) Assessment of groundwater resources in selected areas of Al Ain in the UAE. M.Sc. thesis, United Arab Emirates University, Al Ain
- Alfaro P, Liesch T, Goldscheider N (2017) Modelling groundwater over-extraction in the southern Jordan Valley with scarce data. *Hydrogeol J* 25(5):1319–1340
- Alsharhan AS, Rizk ZA, Nairn AEM, Bakhit DW, Alhajari (2001) Hydrogeology of an arid region. The Arabian Gulf and adjoining areas. Elsevier, New York
- Anderson MP, Woessner WW, Hunt RJ (2015) Applied groundwater modeling: simulation of flow and advective transport. Academic Press, New York
- Brook M (2009) Water resources of Abu Dhabi Emirate, UAE. Water Resources Department, Environment Agency Abu Dhabi, Abu Dhabi
- de Graaf IEM, van Beek RLP., Gleeson T, Moosdorf N, Schmitz O, Sutanudjaja EH, Bierkens MFP (2017) A global-scale two-layer transient groundwater model: development and application to groundwater depletion. *Adv Water Res* 102:53–67
- Dougherty WW, Fencel A, Elasha BO, Swartz C, Yates D, Fisher J, Klein R (2009) Climate change impacts, vulnerability and adaptation. Environmental Agency Abu Dhabi, Abu Dhabi
- EAD (2012) Advancing sustainable groundwater management in Abu Dhabi. Environment Agency Abu Dhabi, UAE, p 3
- Elmahdy S, Mohamed M (2012) Topographic attributes control groundwater flow and groundwater salinity of Al Ain, UAE: a prediction method using remote sensing and GIS. *J Environ Earth Sci* 2(8):1–13
- Elmahdy S, Mohamed M (2013a) Influence of geological structures on groundwater accumulation and groundwater salinity in Northern UAE. *Geocarto Int* 28:453–472
- Elmahdy S, Mohamed M (2013b) Remote sensing and GIS applications of surface and near-surface hydromorphological features in Darfur region, Sudan. *Int J Remote Sens* 34(13):4715–4735
- Elmahdy S, Mohamed M (2014a) Groundwater potential modeling using remote sensing and GIS: a case study of the Al Dhaid area, United Arab Emirates. *Geocarto Int* 29:433–450
- Elmahdy S, Mohamed M (2014b) Relationship between geological structures and groundwater flow and groundwater salinity in Al Ain, UAE; mapping and analysis by means of remote sensing and GIS. *Arab J Geosci* 7(3):1249–1259
- Elmahdy S, Mohamed M (2015a) Automatic detection of near surface geological and hydrological features and investigating their influence on groundwater accumulation and salinity in southwest Egypt using remote sensing and GIS. *Geocarto Int* 30(2):132–144
- Elmahdy S, Mohamed M (2015b) Probabilistic frequency ratio model for groundwater potential mapping in Al Jaww plain, UAE. *Arab J Geosci* 8(4):2405–2416
- ERWDA (2001) Al Wathba Wetland Reserve Management Plan. Internal Report NO. EP0347. ERWDA Library, Abu Dhabi
- Ferre TPA, Thomossan MJ (2010) Understanding the impacts of anisotropy on the extend of drawdown. *Groundwater* 48(4):478–479. <https://doi.org/10.1111/j.1745-6584.2009.00656.x>
- Frenken K (2008) Irrigation in the middle east region in figures AQUASTAT survey-2008. Food and Agriculture Organization of the United Nations, Rome, Italy
- Gascuel Odoux C, Weiler M, Molenat J (2010) Effect of the spatial distribution of physical aquifer properties on modeled water table depth and stream discharge in a headwater catchment. *Hydro Earth Syst Sci* 14(7):1179–1194. <https://doi.org/10.5194/hess-14-1179-2010>
- Gates TK, Garcia LA, Hemphill RA, Morway ED, Elhaddad A (2012) Irrigation practices, water consumption, and return flows in Colorado's lower Arkansas River Valley field and model investigations. Colorado Water Institute, Colorado State University, Fort Collins
- Gebreyohannes T, De Smedt F, Walraevens K, Gebresilassie S, Hussien A, Hagos M, Amare K, Deckers J, Gebrehiwot K (2017). Regional groundwater flow modeling of the Geba basin, northern Ethiopia. *Hydrogeol J*, 25(3):639–655
- Haitjema H (2006) The role of hand calculations in groundwater flow modeling. *Groundwater* 44(6):786–791
- Halcrow SW, Partners (1969) Report on the water resources of the TRUCIAL states. Engineering report for the Trucial States Council. Water Resources Survey, Ministry of Agriculture and Fisheries, Dubai
- Harbaugh AW (2005) MODFLOW-2005, The U.S. Geological Survey's Modular Groundwater Flow Model. The Groundwater Flow Process: U.S. Geological Survey Techniques and Methods 6-A16. U.S. Geological Survey, Reston
- Hassan A, Mohamed M (2003) On using particle tracking method to simulate transport in single continuum and dual continua porous media. *J Hydrol* 275(3–4):242–260
- Havril T, Tóth A, Molson JW, Galsa A, Mádl-Szőnyi J (2017) Impacts of predicted climate change on groundwater flow systems: can wetlands disappear due to recharge reduction? *J Hydrol*. <https://doi.org/10.1016/j.jhydrol.2017.09.020>
- Healy RW (2010) Estimating groundwater recharge. Contribution by Scanlon B. R., Cambridge University Press. Cambridge
- Healy RW, Cook PG (2002) Using groundwater levels to estimate recharge. *Hydrogeol J* 10(1):91–109. <https://doi.org/10.1007/s10040-001-0178-0>
- Hill MC, Tiedeman CR (2006) Effective groundwater model calibration: with analysis of data, sensitivities, predictions, and uncertainty. Wiley, New York. <https://doi.org/10.1002/0470041080>
- Howell TA (2003) Encyclopedia of water science. Marcel Dekker, Inc, New York
- IPCC (2007) IPCC, 2007: climate change 2007: impacts, adaptation and vulnerability. In: Contribution of working group II to the fourth assessment report of the intergovernmental panel on climate change
- Jassas H, Merkel B (2014) Estimating groundwater recharge in the semiarid Al-Khazir Gomal Basin, North Iraq. *Water* 6(8):2467–2481. <https://doi.org/10.3390/w6082467>
- Jinyu S, Qiang Z, Mo X (2010) Regional groundwater flow modeling of Yarkant basin in West China. In: Proceedings: Conference on environmental pollution and public health 2010, 10–11 Sept 2010, Wuhan, China

- Khalifa AA (1995) Surface water and groundwater resources in United Arab Emirates: Culture and Science Society. In: Meeting on Water balance in United Arab Emirates, Dubai
- Khan IA (1980) Determining impact of irrigation on groundwater. *J Irrig Drain Eng* 106(IR4):331–344
- Konikow LF (2011) The secret to successful solute-transport modeling. *Groundwater* 49(2):144–159. <https://doi.org/10.1111/j.1745-6584.2010.00764.x>
- Miller CT, Dawson CN, Farthing MW, Hou TY, Huang J, Kees CE, Kelley CT, Langtangen HP (2013) Numerical simulation of water resources problems: models, methods, and trends. *Adv Water Res* 51:405–437
- MoE (2006) Initial National Communication to the United Nations Framework Convention on Climate Change. Ministry of Energy, United Arab Emirates
- MoE (2015) The UAE state of energy report. Ministry of Energy, United Arab Emirates
- Mohamed M (2014) An integrated water resources management strategy for Al-Ain City, United Arab Emirates. *Proc Int Assoc Hydrol Sci* 364:273–278
- Mohamed M, Almualla A (2010a) Water demand forecasting in Umm Al-Quwain (UAE) using the IWR-MAIN Specify Forecasting Model. *Water Resour Manag* 24:4093–4120
- Mohamed M, Almualla A (2010b) Water demand forecasting in Umm Al-Quwain using the constant rate model. *Desalination* 259:161–186
- Mohamed M, Hatfield K (2005) Modeling microbial-mediated reduction in batch reactors. *Chemosphere* 59(8):1207–1217
- Mohamed M, Hatfield K, Hassan AE (2006) Monte Carlo evaluation of microbial-mediated contaminant reactions in heterogeneous aquifers. *Adv Water Resour* 29(8):1123–1139
- Mohamed M, Hatfield K, Perminova IV (2007) Evaluation of the monod kinetic parameters in the subsurface using moment analysis: theory and numerical testing. *Adv Water Resour* 30(9):2034–2050
- Mohamed M, Saleh N, Sherif M (2010a) Modeling in-situ benzene bioremediation in the contaminated liwa aquifer (UAE) using the slow-release oxygen source technique. *Environ Earth Sci* 61(7):1385–1399
- Mohamed M, Saleh N, Sherif M (2010b) Sensitivity of natural attenuation to variations in kinetic and transport parameters. *Bull Environ Contam Toxicol* 84:443–449
- MWR (1999) Ministry of Water Resources, Sultanate of Oman, Water Attachment position paper
- Osterkamp WR, Lane LJ, Menges CM (1995) Techniques of groundwater recharge estimates in arid/semi-arid areas, with examples from Abu Dhabi. *J Arid Environ* 31(3):349–369
- PIK (2007) Development of functional irrigation types for improved global crop modelling. Potsdam Institute for Climate Impact Research (PIK). PIK Report no. 104. Potsdam, March 2007
- Poeter EP, Hill MC (1997) Inverse models: a necessary next step in groundwater modeling. *Groundwater* 35(2):250–260
- Reilly TE, Harbaugh AW (1993) Computer note: simulation of cylindrical flow to a well using the U.S. Geological Survey modular finite-difference ground-water flow model. *Groundwater* 31(3):489–494
- Rizk ZS, Alsharhan AS (2003) Water resources in the United Arab Emirates. In: Alsharhan AS, Wood WW (eds) Water resources perspectives: evaluation, management and policy. Elsevier Science, Amsterdam, pp 245–264
- Rizk ZS, Garamoon HK, El Etr HA (1998b) Morphometry, surface runoff and flood potential of major drainage basins of Al Ain Area, United Arab Emirates. *Egypt J Remote Sens Sp Sci* 1(1):369–390
- Sahoo S, Jha MK (2017) Numerical groundwater-flow modeling to evaluate potential effects of pumping and recharge: implications for sustainable groundwater management in the Mahanadi delta region, India. *Hydrogeol J* 25(8):2489–2511
- Saroli M, Lancia M, Albano M, Casale A, Giovinco G, Petitta M, Zarlenga F, Dell'Isola M (2017) A hydrogeological conceptual model of the Suio hydrothermal area (central Italy). *Hydrogeol J* 25(6):1811–1832
- Sathish S, Elango L (2015) Numerical simulation and prediction of groundwater flow in a coastal aquifer of Southern India. *J Water Resour Prot* 7(17):1483–1494. <https://doi.org/10.4236/jwarp.2015.717122>
- Sathish S, Mohamed MM (2018) Assessment of aquifer storage and recovery (ASR) feasibility at selected sites in the Emirate of Abu Dhabi, UAE. *Environ Earth Sci* 77:112. <https://doi.org/10.1007/s12665-018-7251-7>
- SCAD (2011) Water Statistics. Statistic Centre-Abu Dhabi. Access date 14 March 2016
- Shahid SA, Taha FK, Abdelfattah MA (2013) Developments in soil classification, land use planning and policy implications: innovative thinking of soil inventory for land use planning and management of land resources. Springer Science & Business Media, Berlin
- Sherif M, Mohamed M, Shetty A, Almulla M (2011a) Rainfall-runoff modeling of three wadis in the northern area of UAE. *J Hydrol Eng (ASCE)* 16:10–20
- Sherif M, Mohamed M, Kacimov A, Shetty A (2011b) Assessment of groundwater quality in the northeastern coastal area of UAE as precursor for desalination. *Desalination* 273:436–446
- Siarkos I, Latinopoulos P (2016) Modeling seawater intrusion in over-exploited aquifers in the absence of sufficient data: application to the aquifer of Nea Moudania, northern Greece. *Hydrogeol J* 24(8):2123–2141
- Stanford WE, Wood WW (2001) Hydrology of the coastal Sabkhas of Abu Dhabi, United Arab Emirates. *Hydrogeol J* 9(4):358–366. <https://doi.org/10.1007/s100400100137>
- Todd DK (1980) Groundwater hydrology, 2nd edn. Wiley, New York
- Townley LR (1995) The response of aquifers to periodic forcing. *Adv Water Resour* 18(3):125–146
- US Geological Survey (1996) Bibliography of national drilling company–United States Geological Survey Reports on the Water Resources of Abu Dhabi Emirate. U.S Geological Survey Open File Report
- Wheater HS, Sorooshian S, Sharma KD (eds) 2008. Hydrological modelling in arid and semi arid areas. Cambridge University Press, Cambridge
- Woodward SJR, Wohling T, Stenger R (2016) Uncertainty in the modeling of spatial and temporal patterns of shallow groundwater flow paths: the role of geological and hydrological site information. *J Hydrol* 534:680–694
- Yang F, Bai B, Dunn-Norman S (2011) Modeling the effects of completion techniques and formation heterogeneity on CO<sub>2</sub> sequestration in shallow and deep saline aquifers. *Environ Earth Sci* 64(3):841–849
- Zeng Y, Xie Z, Yu Y, Liu S, Wang L, Zou J, Qin P, Jia B (2016) Effects of anthropogenic water regulation and groundwater lateral flow on land processes. *J Adv Model Earth Syst* 8(3):1106–1131. <https://doi.org/10.1002/2016MS000646>
- Zhou Y, Li W (2011) A review of regional groundwater flow modeling. *Geosci Front* 2(2):205–214
- Zhou P, Li G, Lu Y, Li M (2014) Numerical modeling of the effects of beach slope on water-table fluctuation in the unconfined aquifer of Donghai Island, China. *Hydrogeol J* 22(2):383–396